Equation of state from lattice QCD

Claudia Ratti

University of Houston

Open Questions

- Is there a critical point in the QCD phase diagram?
- What are the degrees of freedom in the vicinity of the phase transition?
- Where is the transition line at high density?
- What are the phases of QCD at high density?
- Are we creating a thermal medium in experiments?

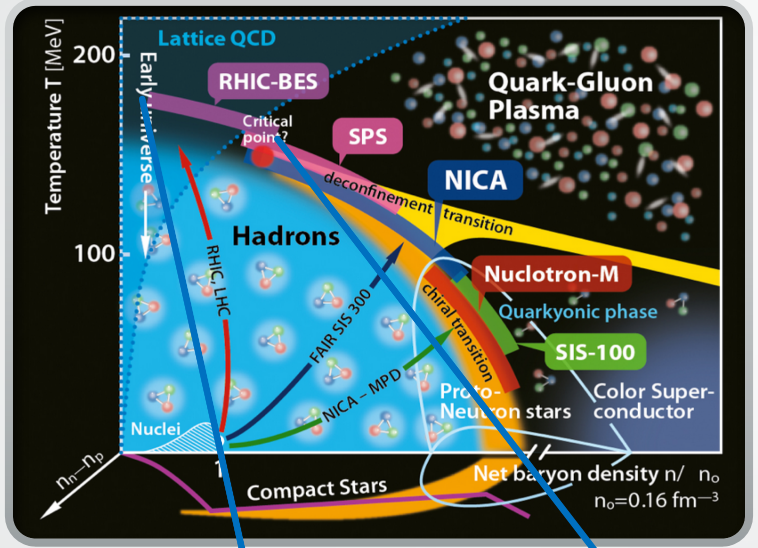

- Run 2019:
  - Collider: $\sqrt{s_{NN}}$=14.6, 19.6, 200 GeV
  - Fixed target: $\sqrt{s_{NN}}$=3.2 GeV
- Run 2020:
  - Collider: $\sqrt{s_{NN}}$=9.2, 11.5 GeV
  - Fixed target: $\sqrt{s_{NN}}$=3.5, 3.9, 4.5, 5.2, 6.2, 7.2, 7.7 GeV
- Run 2021:
  - Collider: $\sqrt{s_{NN}}$=7.7 GeV

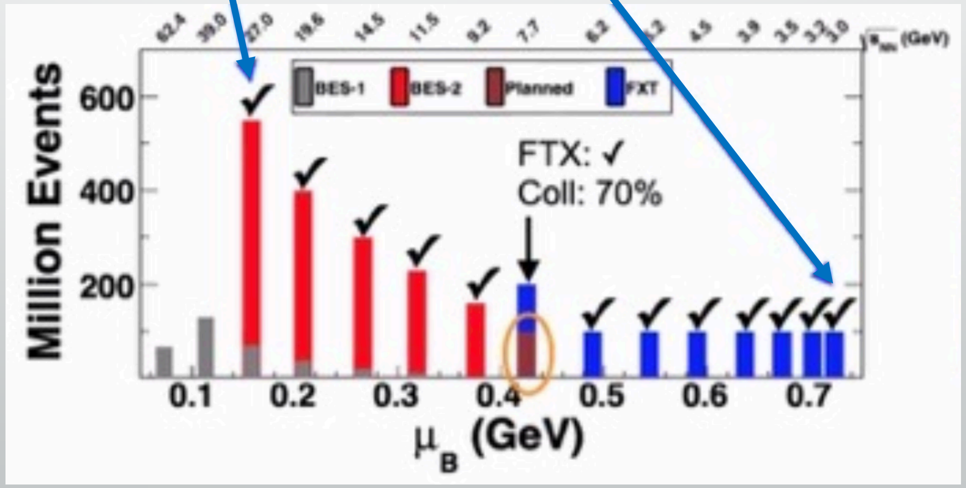

Comparison of the facilities

Compilation by D. Cebra

Facilty	RHIC BESII	SPS	NICA	SIS-100 SIS-300	J-PARC HI
Exp.:	STAR +FXT	NA61	MPD + BM@N	CBM	JHITS
Start:	2019-20 2018	2009	2020 2017	2022	2025
Energy: $\sqrt{s_{NN}}$ (GeV)	7.7– 19.6 2.5-7.7	4.9-17.3	2.7 - 11 2.0-3.5	2.7-8.2	2.0-6.2
Rate: At 8 GeV	100 HZ 2000 Hz	100 HZ	<10 kHz	<10 MHZ	100 MHZ
Physics:	CP&OD	CP&OD	OD&DHM	OD&DHM	OD&DHM
	Collider Fixed target	Fixed target Lighter ion collisions	Collider Fixed target	Fixed target	Fixed target

CP=Critical Point OD= Onset of Deconfinement DHM=Dense Hadronic Matter

How can lattice QCD support the experiments?

- Equation of state
  - Needed for hydrodynamic description of the QGP
- QCD phase diagram
  - Transition line at finite density
  - Constraints on the location of the critical point
- Fluctuations of conserved charges
  - Can be simulated on the lattice and measured in experiments
  - Can give information on the evolution of heavy-ion collisions
  - Can give information on the critical point

QCD Equation of state at finite density from the lattice

QCD EoS at μ_B=0

WB: PLB (2014); HotQCD: PRD (2014)

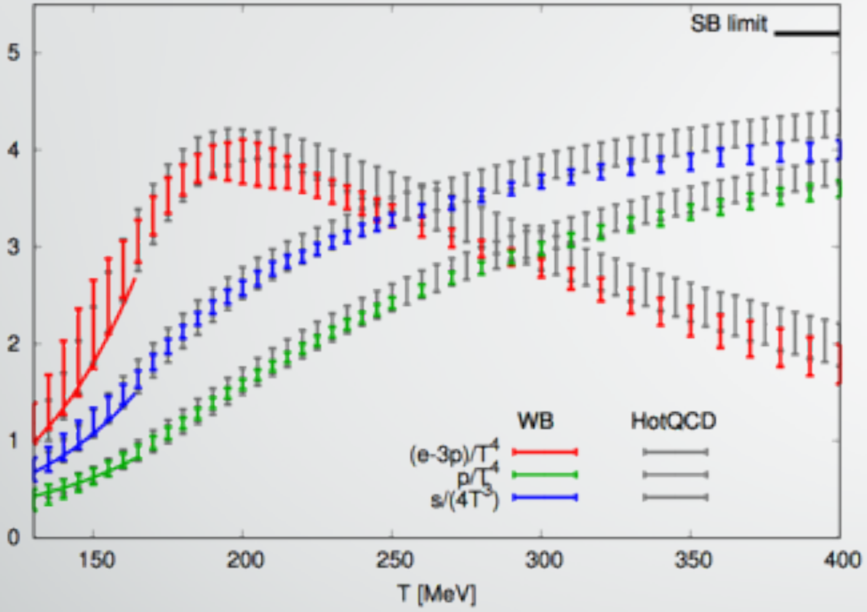

WB: Nature (2016)

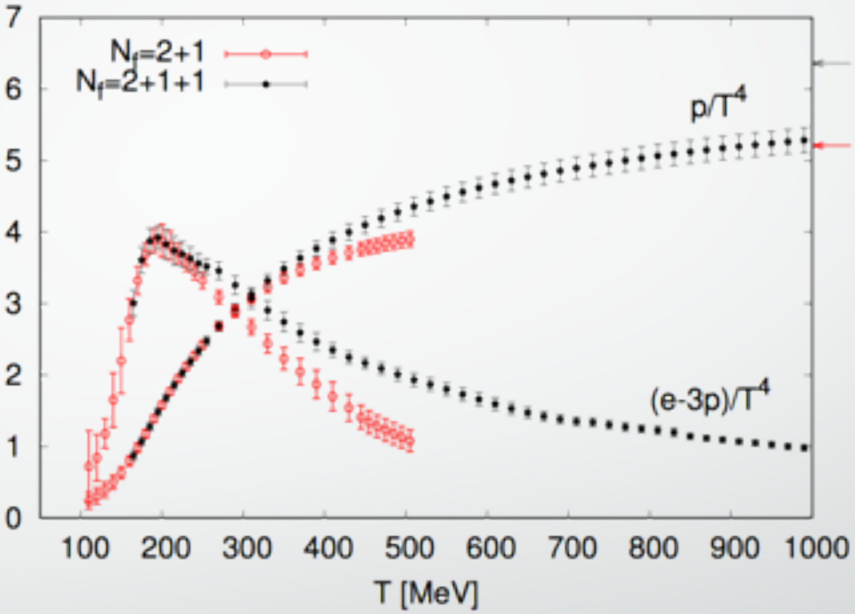

- EoS for N_f=2+1 known in the continuum limit since 2013
- Good agreement with the HRG model at low temperature
- Charm quark relevant degree of freedom already at T~250 MeV

Constraints on the EoS from the experiments

S. Pratt et al., PRL (2015)

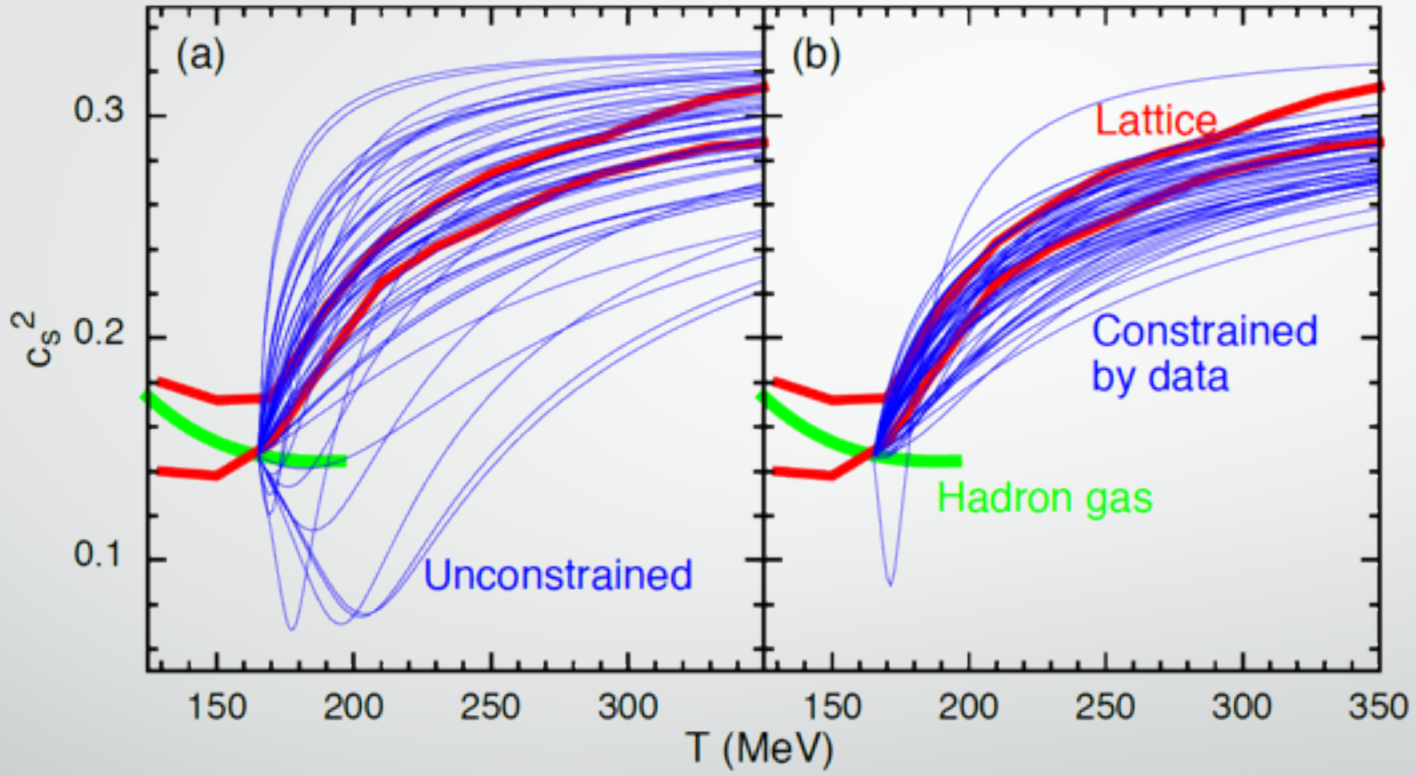

- Comparison of data from RHIC and LHC to theoretical models through Bayesian analysis
- The posterior distribution of EoS is consistent with the lattice QCD one

Taylor expansion of EoS

- Taylor expansion of the pressure:

$$\frac{p(T,\mu_B)}{T^4} = \frac{p(T,0)}{T^4} + \sum_{n=1}^{\infty} \frac{1}{(2n)!} \frac{\mathrm{d}^{2n}(p/T^4)}{d(\frac{\mu_B}{T})^{2n}}\Bigg|_{\mu_B=0} \left(\frac{\mu_B}{T}\right)^{2n} = \sum_{n=0}^{\infty} c_{2n}(T) \left(\frac{\mu_B}{T}\right)^{2n}$$

- Two ways of extracting the Taylor expansion coefficients:
  - Direct simulation
  - Simulations at imaginary μ_B

- Two physics choices:
  - $\mu_B \neq 0$, $\mu_S = \mu_Q = 0$
  - μ_S and μ_Q are functions of T and μ_B to match the experimental constraints:

$\langle n_S \rangle = 0$ $\qquad\qquad$ $\langle n_Q \rangle = 0.4 \langle n_B \rangle$

Range of validity of equation of state

- We now have the equation of state for $\mu_B/T \leq 2$ or in terms of the RHIC energy scan:

$$\sqrt{s} = 200,\ 62.4,\ 39,\ 27,\ 19.6,\ 14.5\mathrm{GeV}$$

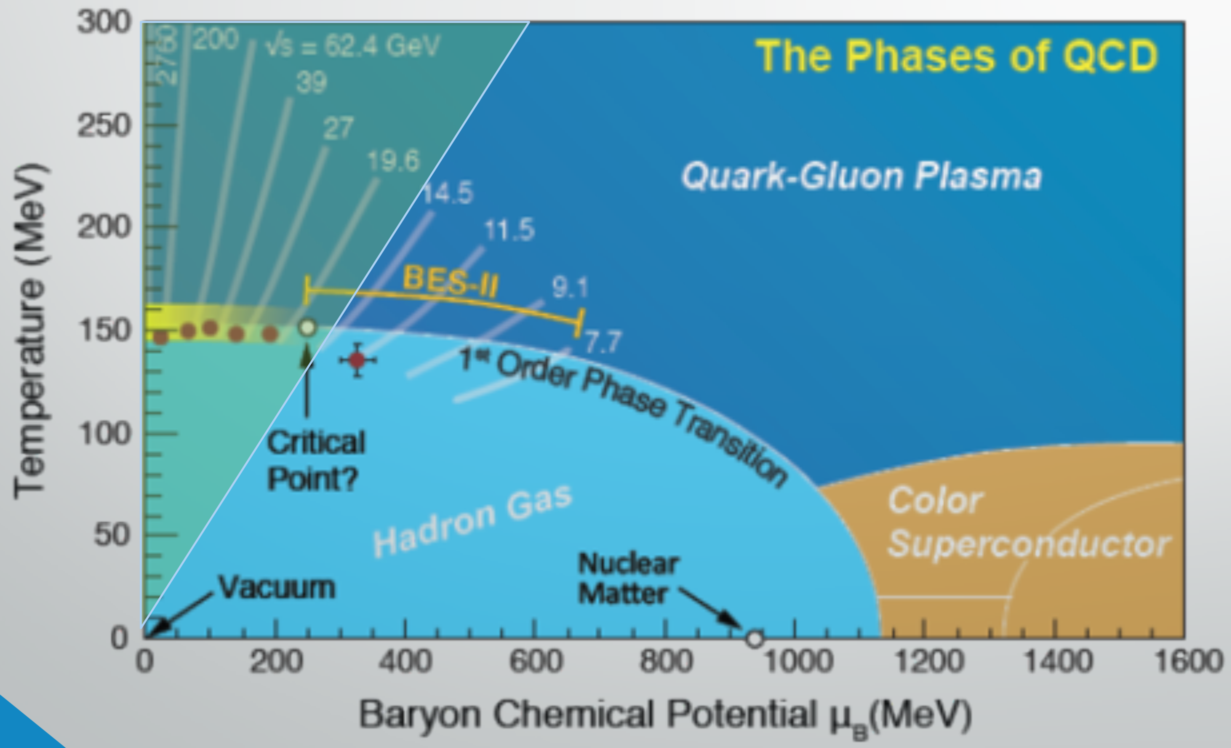

Other expansion schemes have been proposed recently
S. Mukherjee et al., 2021

Introducing a novel expansion scheme

S. Borsanyi, C. R. et al., PRL (2021)

Motivation

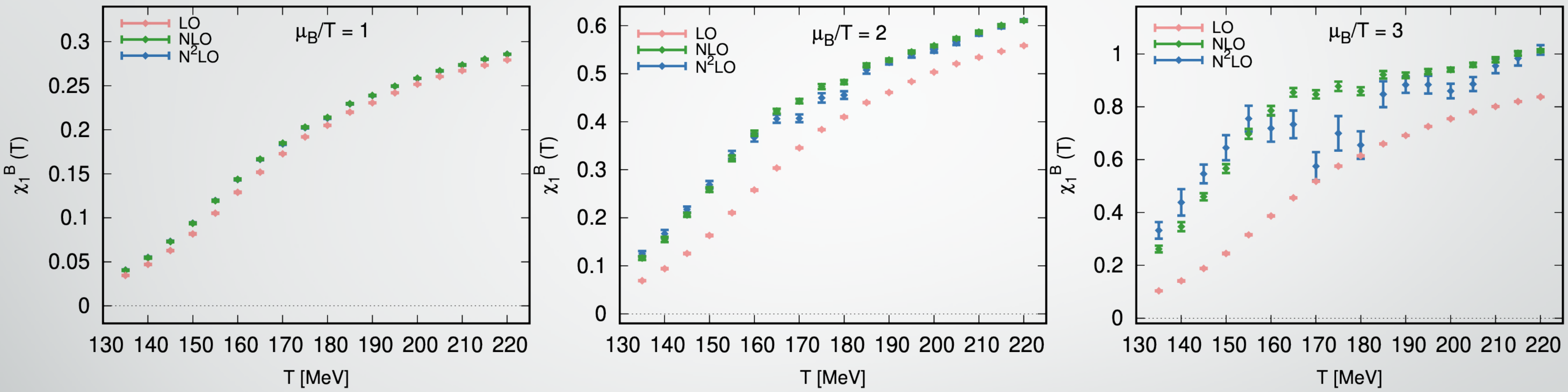

- ❑ Poor convergence of Taylor series: need to sum many terms to reach high μ_B
- ❑ Oscillatory/non-monotonic behavior in some observables at high μ_B
  - ➢ Unphysical, due to truncation of Taylor series

An alternative approach

From simulations at imaginary μ_B we *observe* that $\chi_1^B(T,\hat{\mu}_B)$ at (imaginary) $\hat{\mu}_B$ appears to be differing from $\chi_2^B(T,0)$ mostly by a rescaling of T:

$$\frac{\chi_1^B(T,\hat{\mu}_B)}{\hat{\mu}_B} = \chi_2^B(T',0)\ ,\quad T' = T\left(1+\kappa\,\hat{\mu}_B^2\right)$$

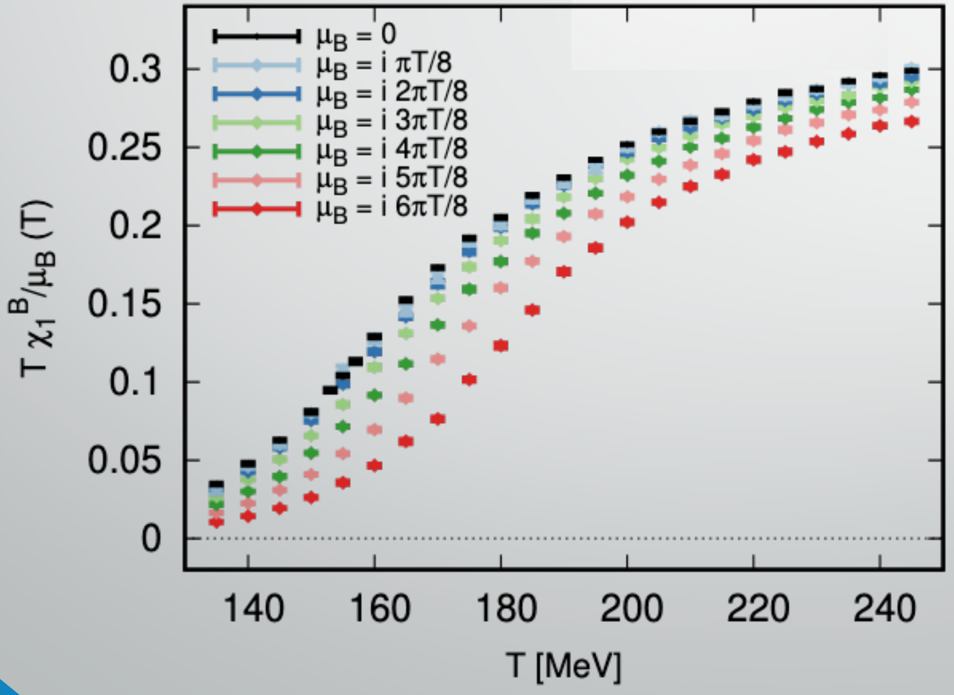

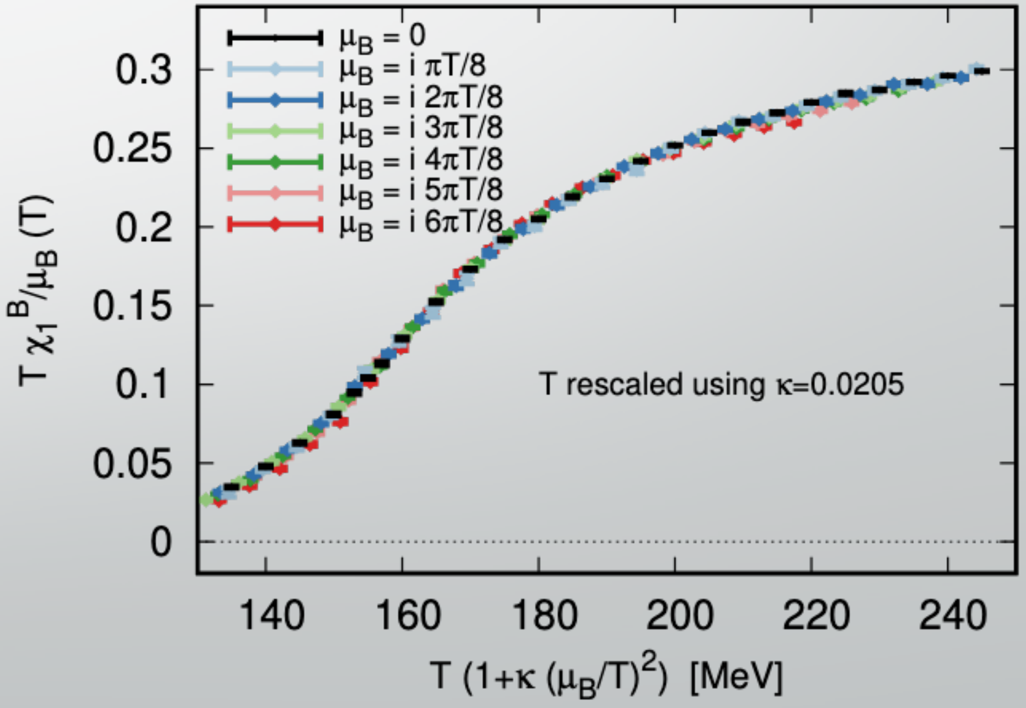

Taylor expanding a (shifting) sigmoid

Assume we have a sigmoid function $f(T)$ which shifts with $\hat{\mu}$, with a simple T-independent shifting parameter κ. How does Taylor cope with it?

$$f(T,\,\hat{\mu}) = f(T',0)\ , \qquad T' = T(1+\kappa\,\hat{\mu}^2)\ ,$$

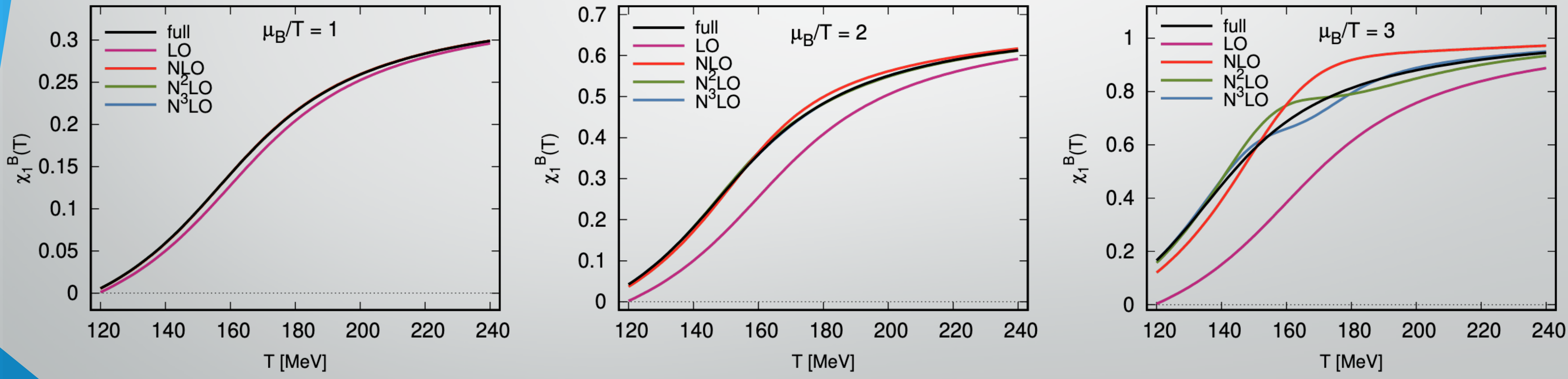

We fitted $f(T,0) = a + b\arctan(c(T-d))$ to $\chi_2^B(T,0)$ data for a 48×12 lattice

Taylor expanding a (shifting) sigmoid

- The Taylor expansion seems to have problems reproducing the original function (left)
- Quite suggestive comparison with actual Taylor-expanded lattice data (right)

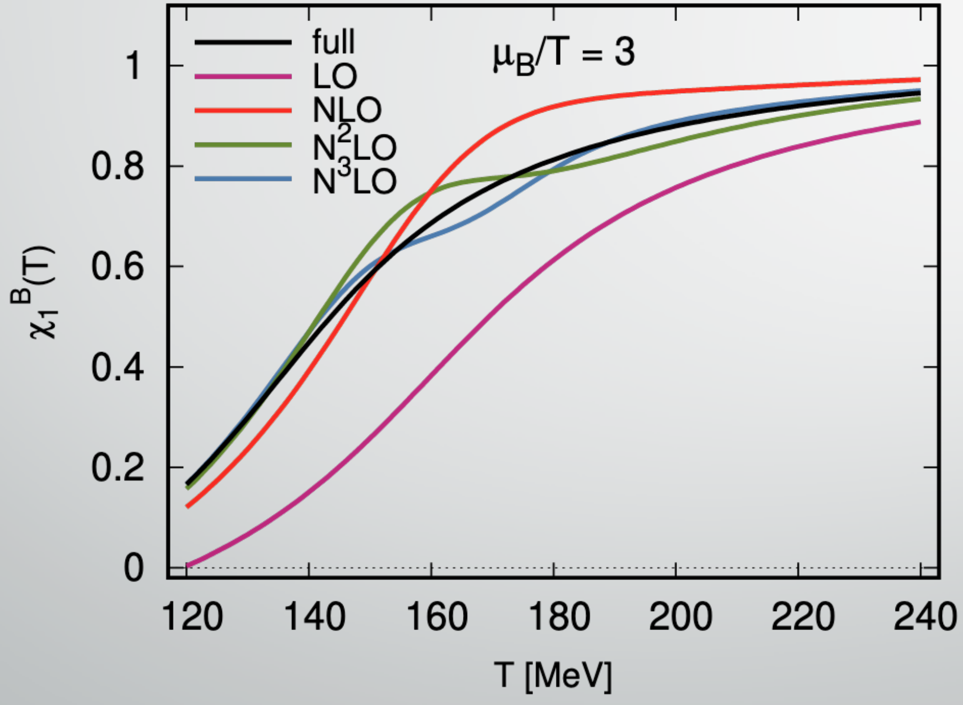

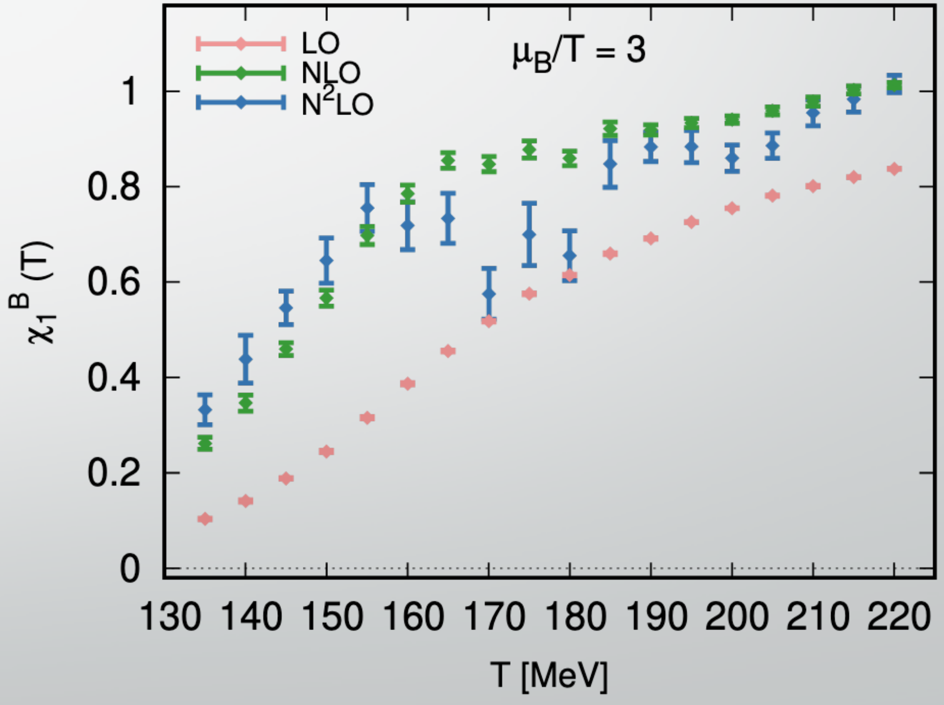

- Problems at T slightly larger than T_{pc} $\Rightarrow$ influence from structure in χ_6^B and χ_8^B

Formulation

- We have observed the $\hat{\mu}_B$-dependence seems to amount to a simple T- rescaling
- A simplistic scenario with a single T- independent parameter κ does not provide a systematic treatment which can serve as an alternative expansion scheme
- We allow for more than $\mathcal{O}(\hat{\mu}^2)$ expansion of T' and let the coefficients be $T-$dependent:

$$\frac{\chi_1^B(T,\hat{\mu}_B)}{\hat{\mu}_B} = \chi_2^B(T',0)\ , \quad T' = T\left(1+\kappa_2(T)\,\hat{\mu}_B^2+\kappa_4(T)\,\hat{\mu}_B^4+\mathcal{O}(\hat{\mu}_B^6)\right)$$

- **Important:** we are simply re-organizing the Taylor expansion via an expansion in the shift

$$\Delta T = T - T' = \left(\kappa_2(T)\,\hat{\mu}_B^2+\kappa_4(T)\,\hat{\mu}_B^4+\mathcal{O}(\hat{\mu}_B^6)\right)$$

- Comparing the (Taylor) expansion in $\hat{\mu}_B$ and our expansion in ΔT order by order, we can relate $\chi_n^B(T)$ and $\kappa_n(T)$

Formulation

- Equating same-order terms, we find

$$\chi_4^B(T) = 6T\kappa_2^{BB}(T)\frac{d\chi_2}{dT} \ ,$$

$$\chi_6^B(T) = 60T^2(\kappa_2^{BB})^2(T)\frac{d^2\chi_2}{dT^2} + 120T\kappa_4^{BB}(T)\frac{d\chi_2}{dT}$$

or, analogously:

$$\kappa_2^{BB}(T) = \frac{1}{6T}\frac{\chi_4^B(T)}{\chi_2^{B\prime}(T)} \ ,$$

$$\kappa_4^{BB}(T) = \frac{1}{360\chi_2^{B\prime}(T)^3}\left(3\chi_2^{B\prime}(T)^2\chi_6^B(T) - 5\chi_2^{B\prime\prime}(T)\chi_4^B(T)^2\right)$$

Analysis

I. Directly determine $\kappa_2(T)$ at $\hat{\mu}_B = 0$ from the previous relation

II. From our imaginary-$\hat{\mu}_B$ simulations ($\hat{\mu}_Q = \hat{\mu}_S = 0$) we calculate:

$$\frac{T' - T}{T\,\hat{\mu}_B^2} = \kappa_2(T) + \kappa_4(T)\,\hat{\mu}_B^2 + \mathcal{O}(\hat{\mu}_B^4) = \Pi(T)$$

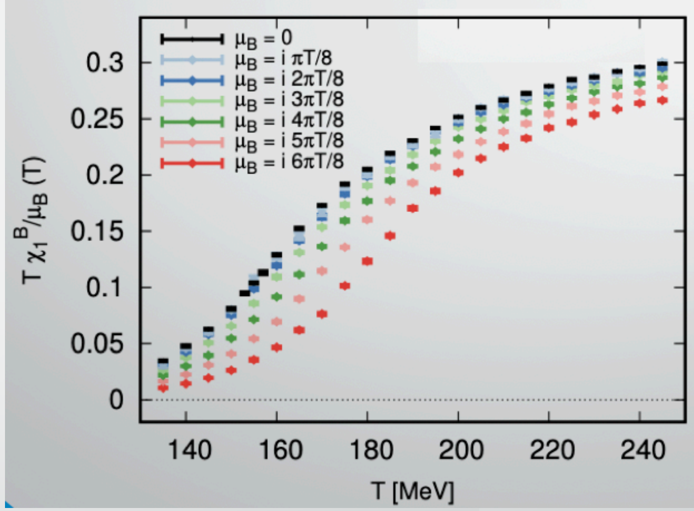

III. Calculate $\Pi(T, N_\tau, \hat{\mu}_B^2)$ for $\hat{\mu}_B = in\pi/8$ and $N_\tau = 10, 12, 16$

IV. Perform a combined fit of the $\hat{\mu}_B^2$ and $1/N_\tau^2$ dependence of $\Pi(T)$ at each temperature, yielding a continuum estimate for the coefficients

$\Rightarrow$ The $\mathcal{O}(1)$ and $\mathcal{O}(\hat{\mu}_B^2)$ coefficients of the fit are $\kappa_2(T)$ and $\kappa_4(T)$

Results for the coefficients

Our initial guess was not far-off:

- Fairly constant $\kappa_2(T)$ over a large T-range
- Clear separation in magnitude between $\kappa_2(T)$ and $\kappa_4(T)$ hints at better convergence
- Agreement with the HRG model results at low temperatures
- Polynomial fits of $\kappa_2(T)$ and $\kappa_4(T)$ before use in thermodynamics (good fit qualities)

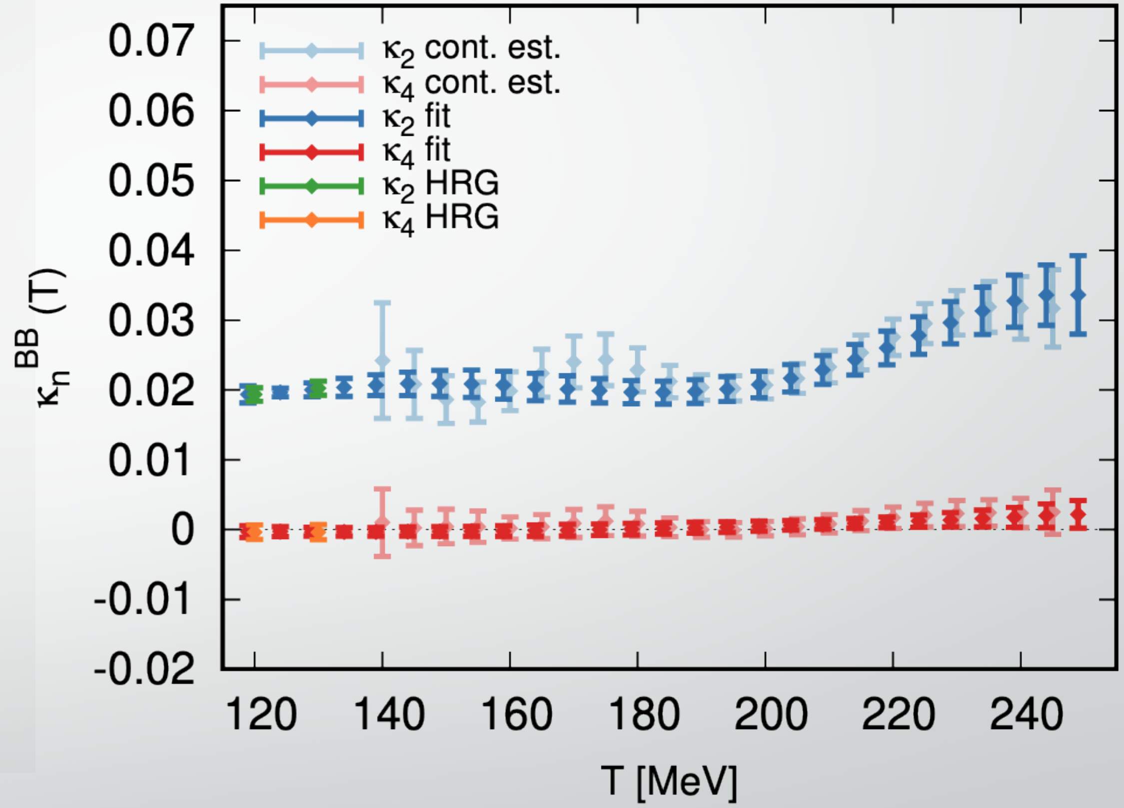

NOTE: polynomial fits take into account both statistical and systematic correlations.

Constructing the density at finite μ_B

We use the following expression:

$$\frac{\chi_1^B(T,\hat{\mu}_B)}{\hat{\mu}_B} = \chi_2^B(T',0) \ ,$$ with

$$T'(T,\hat{\mu}_B) = T\left(1 + \kappa_2^{BB}(T)\hat{\mu}_B^2 + \kappa_4^{BB}(T)\hat{\mu}_B^4 + \mathcal{O}(\hat{\mu}_B^6)\right)$$

We need a continuum result for $\chi_2^B(T,0)$

For some observables such as the entropy, we also need the derivative of $\chi_2^B(T,0)$ with respect to the temperature

Constructing the density at finite μ_B

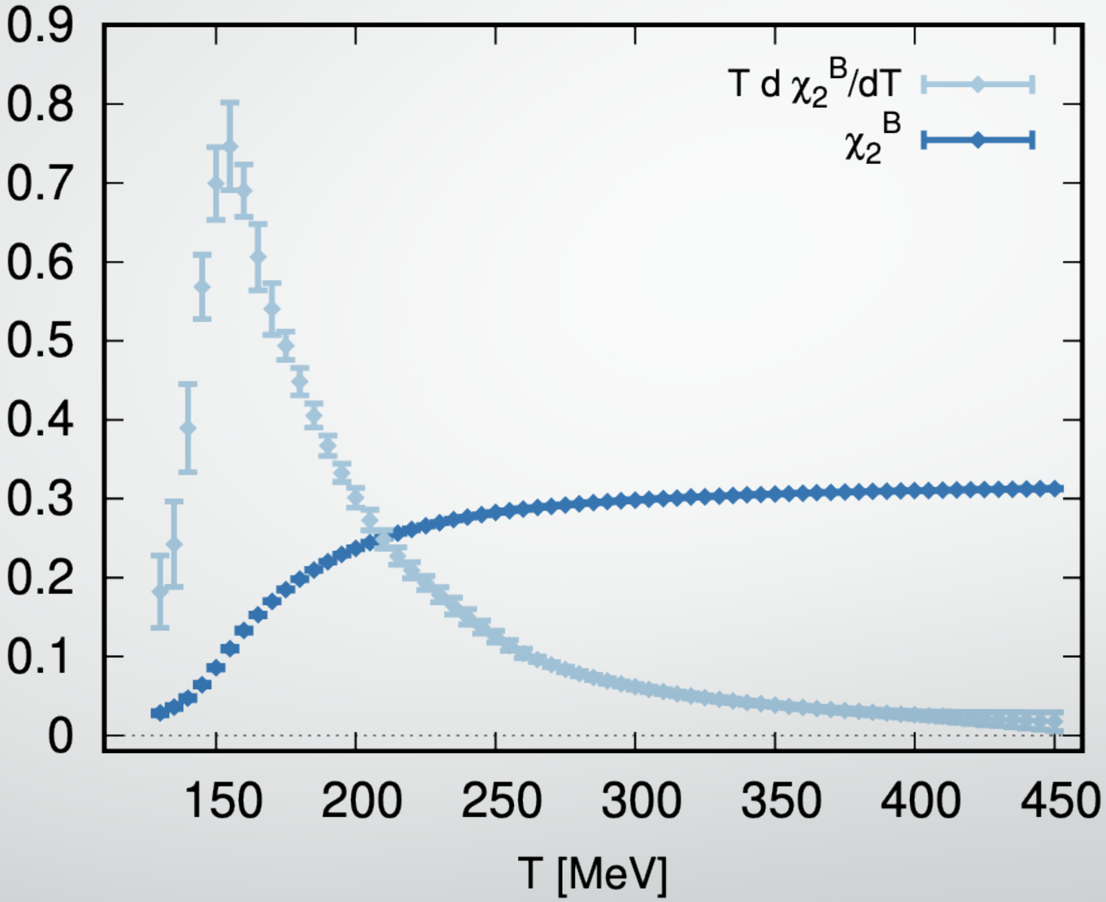

With this result and the set of κ_{ij} coefficients, we can now calculate all thermodynamic quantities

Thermodynamics at finite μ_B

Thermodynamic quantities at finite (real) μ_B can be reconstruted from the same ansazt:

$$\frac{n_B(T,\hat{\mu}_B)}{T^3} = \hat{\mu}_B \chi_2^B(T',0)$$

with $T' = T(1 + \kappa_2^{BB}(T)\,\hat{\mu}_B^2 + \kappa_4^{BB}(T)\,\hat{\mu}_B^4)$.

From the baryon density n_B one finds the pressure:

$$\frac{p(T,\hat{\mu}_B)}{T^4} = \frac{p(T,0)}{T^4} + \int_0^{\hat{\mu}_B} \mathrm{d}\hat{\mu}'_B \, \frac{n_B(T,\hat{\mu}'_B)}{T^3}$$

then the entropy, energy density:

$$\frac{s(T,\hat{\mu}_B)}{T^4} = 4\frac{p(T,\hat{\mu}_B)}{T^4} + T\left.\frac{\partial p(T,\hat{\mu}_B)}{\partial T}\right|_{\hat{\mu}_B} - \hat{\mu}_B\frac{n_B(T,\hat{\mu}_B)}{T^3}$$

$$\frac{\epsilon(T,\hat{\mu}_B)}{T^4} = \frac{s(T,\hat{\mu}_B)}{T^3} - \frac{p(T,\hat{\mu}_B)}{T^4} + \hat{\mu}_B\frac{n_B(T,\hat{\mu}_B)}{T^3}$$

Thermodynamics at finite μ_B: results

- We reconstruct thermodynamic quantities up to $\hat{\mu}_B \simeq 3.5$ with uncertainties well under control
- Agreement with HRG model calculations at small temperatures
- No pathological (non-monotonic) behavior is present

S. Borsanyi, C. R. et al., PRL (2021)

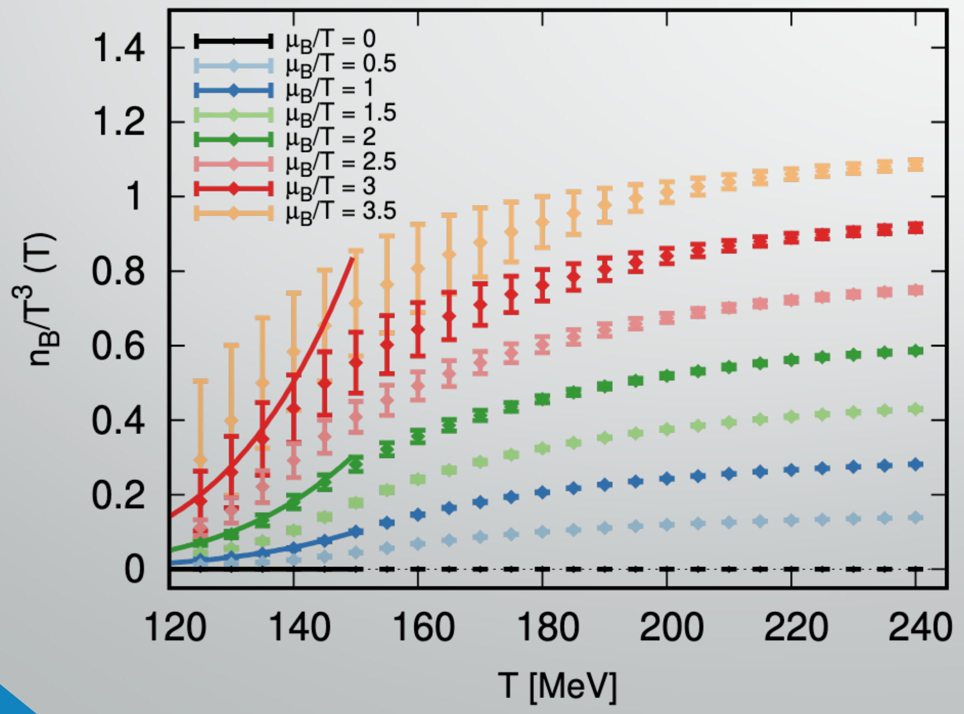

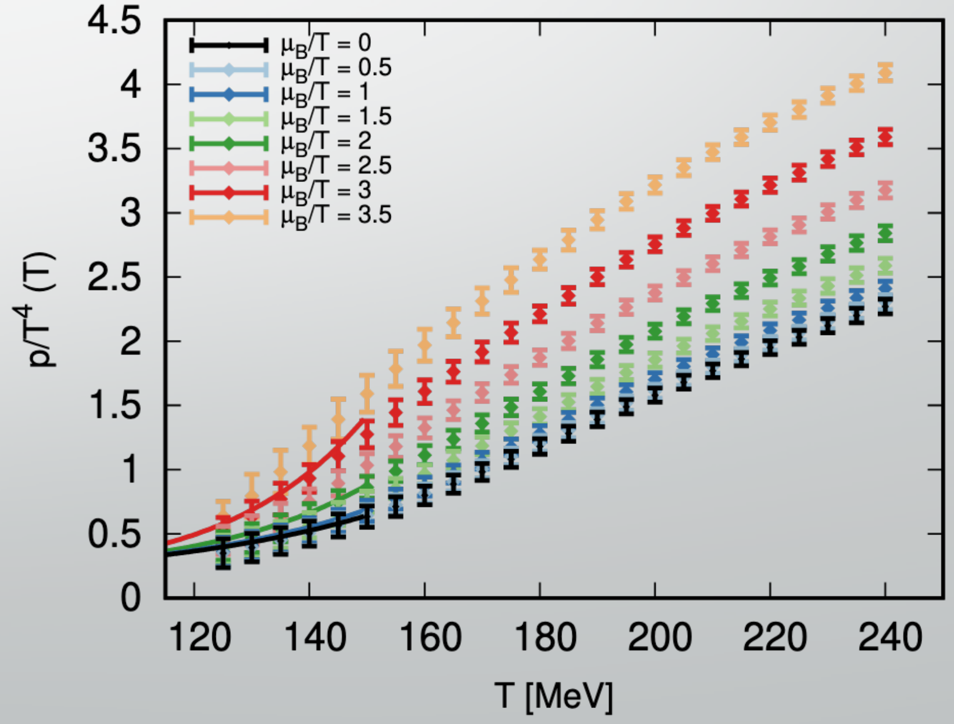

Thermodynamics at finite μ_B: results

- We reconstruct thermodynamic quantities up to $\hat{\mu}_B \simeq 3.5$ with uncertainties well under control
- Agreement with HRG model calculations at small temperatures
- No pathological (non-monotonic) behavior is present

S. Borsanyi, C. R. et al., PRL (2021)

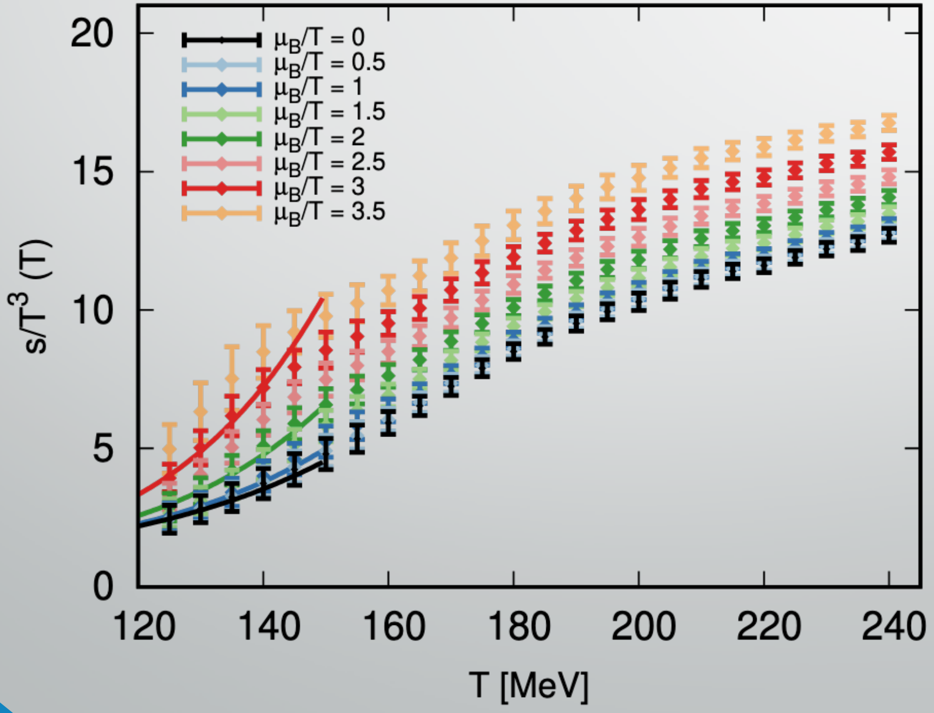

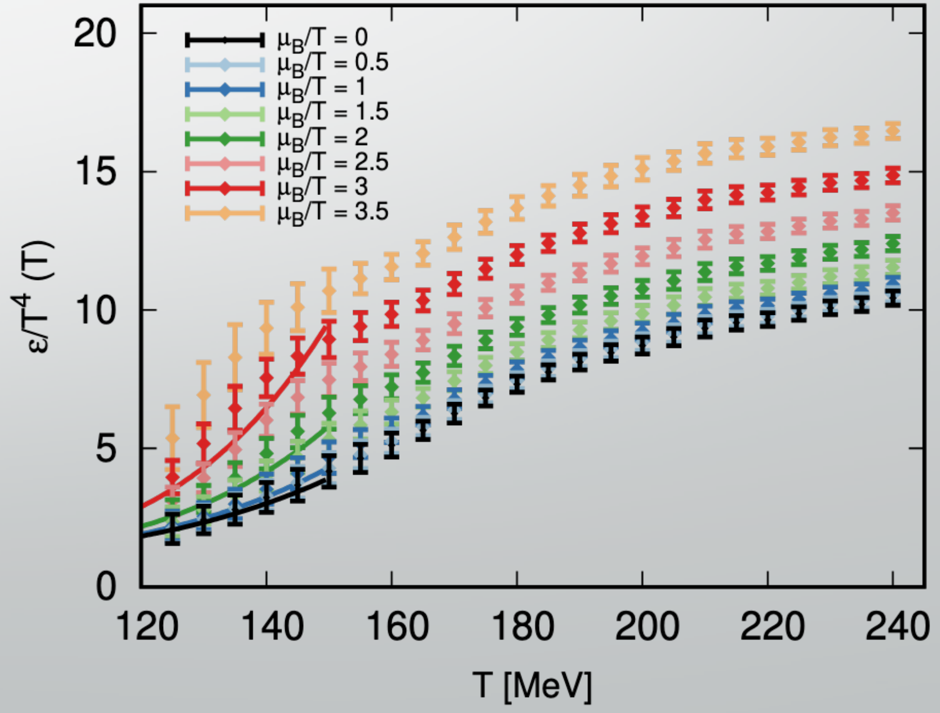

Convergence check

- We also check the results without the inclusion of $\kappa_4(T)$ (darker shades)
- Including $\kappa_4(T)$ only results in added error, but does not "move" the results

$\longrightarrow$ <u>Good convergence</u>

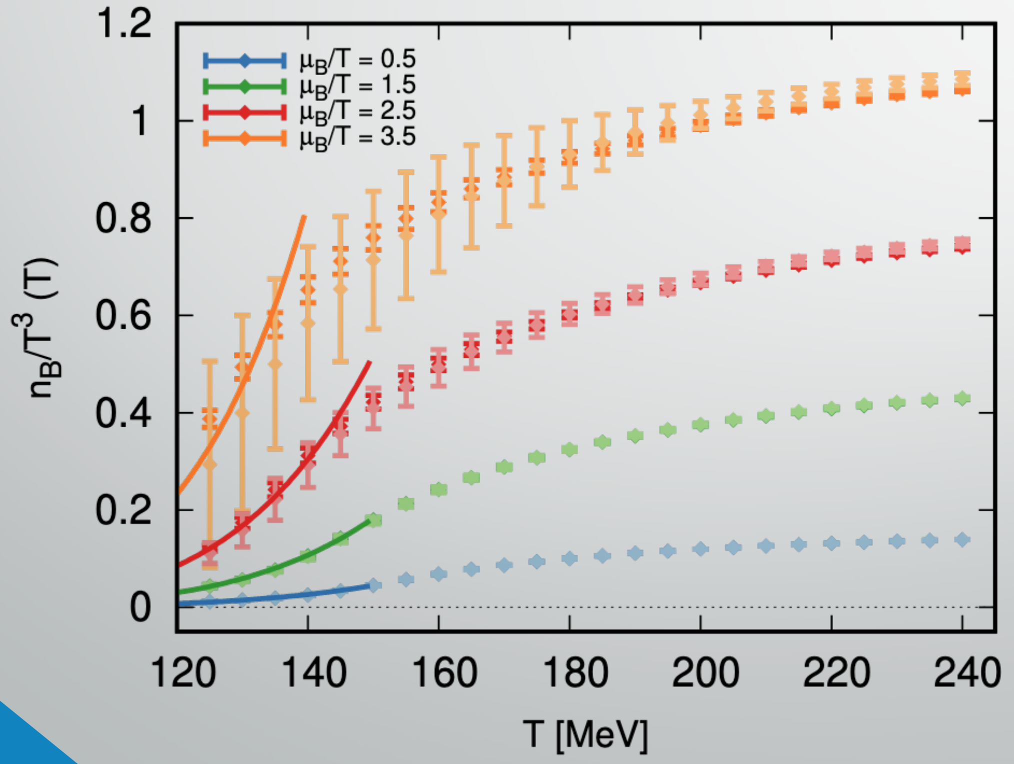

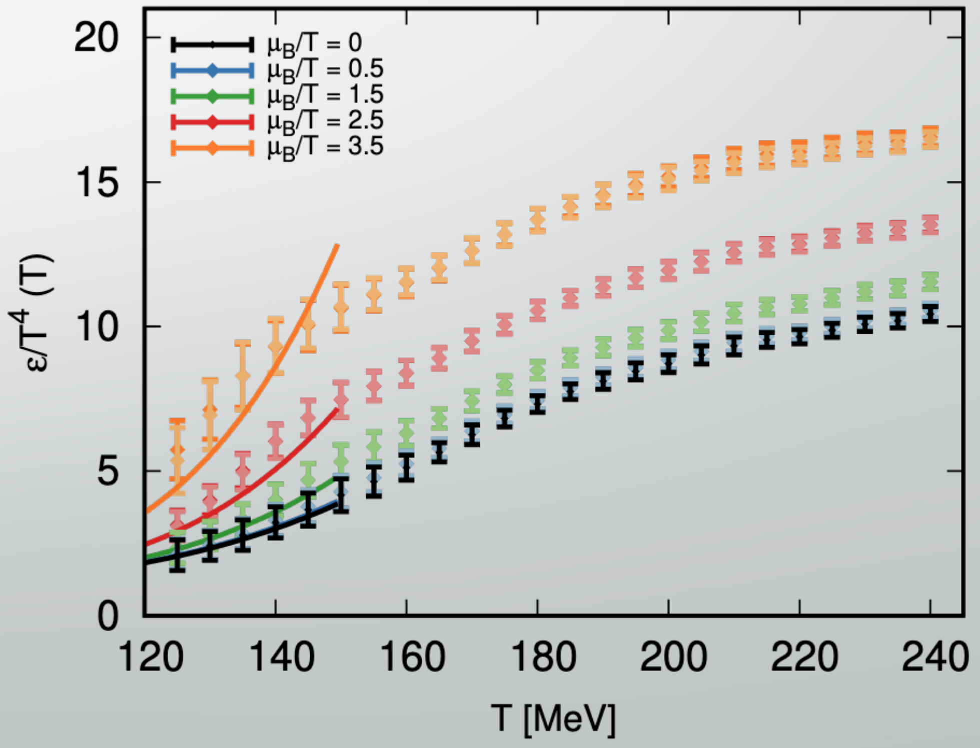

New result: strangeness-neutral EoS and beyond

- We recently extended these results to the case of strangeness-neutrality
- We expand along the strangeness-neutral line in the 4D phase diagram
- We also consider fluctuations of strangeness around the $\langle n_S \rangle = 0$ condition

S. Borsanyi, C. R. et al., 2202.05574

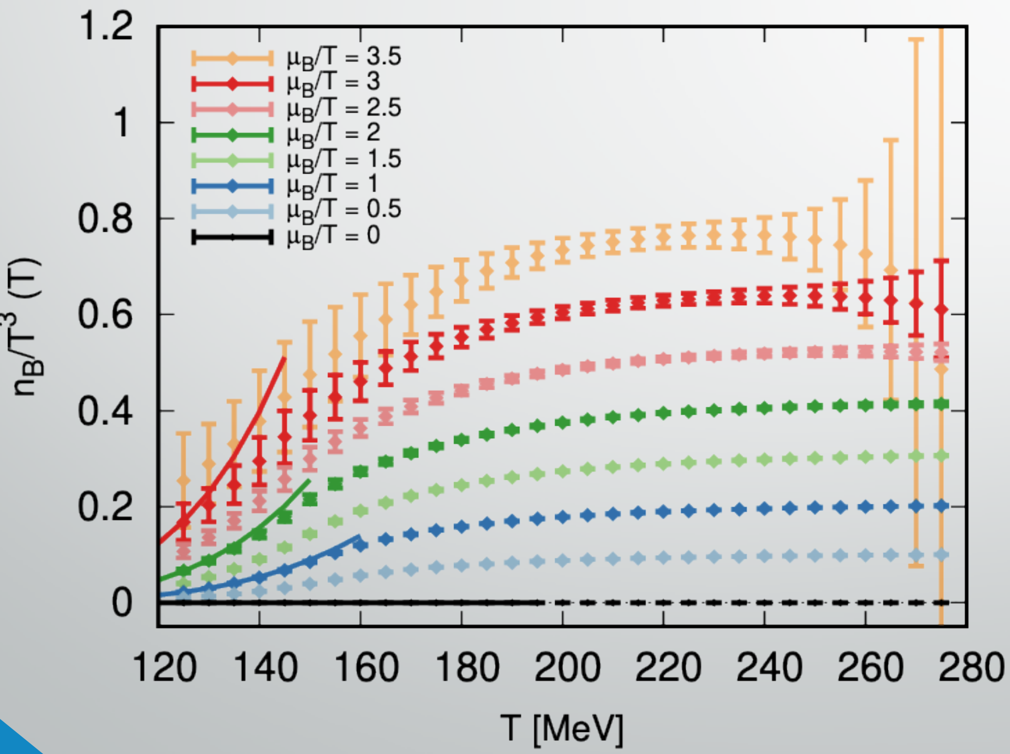

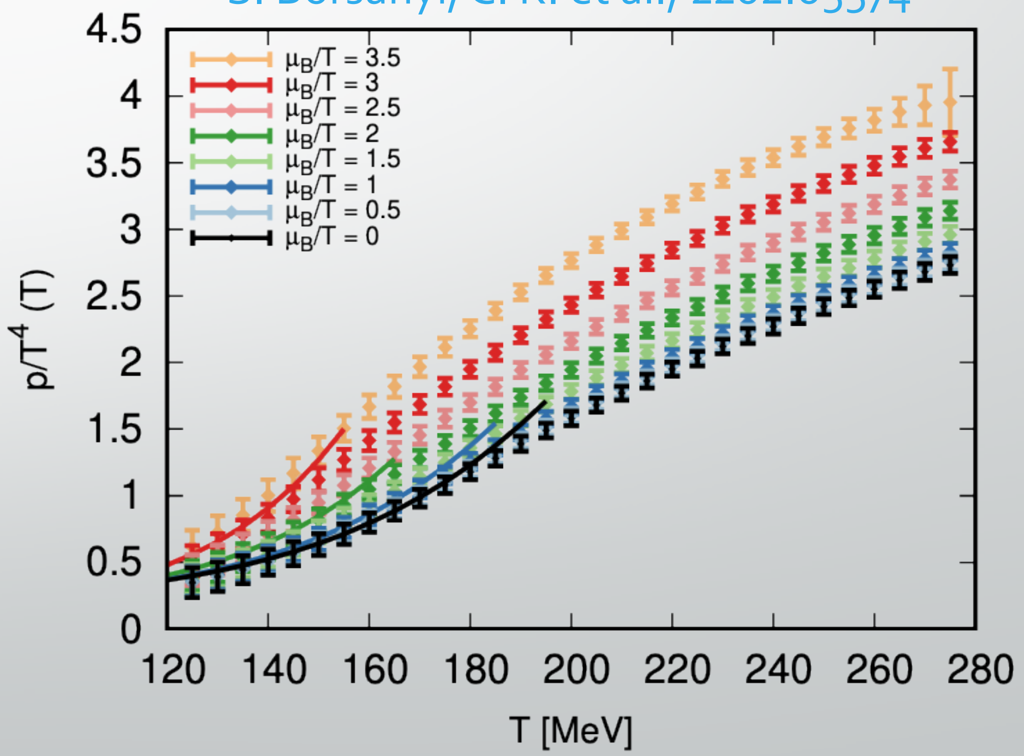

Conclusions

- The EoS for QCD at large chemical potential is highly demanded in heavy-ion collisions community, especially for hydrodynamic simulations
- Historical approach of Taylor expansion for EoS has shortcomings
  - Because of technical/numerical challenges
  - Because of phase structure of the theory
- An alternative expansion scheme tailored to the specific behavior of relevant observables seems a better approach (better convergence)
- Thermodynamic quantities up to $\hat{\mu}_B \simeq 3.5$ have very reasonable uncertainties
- Just like Taylor, systematically improvable

Expansion coefficients

Extract the "regular" contribution as the difference between the lattice and Ising ones

$$T^4 c_n^{\mathrm{LAT}}(T) = T^4 c_n^{\text{Non-Ising}}(T) + T_C^4 c_n^{\mathrm{Ising}}(T)$$

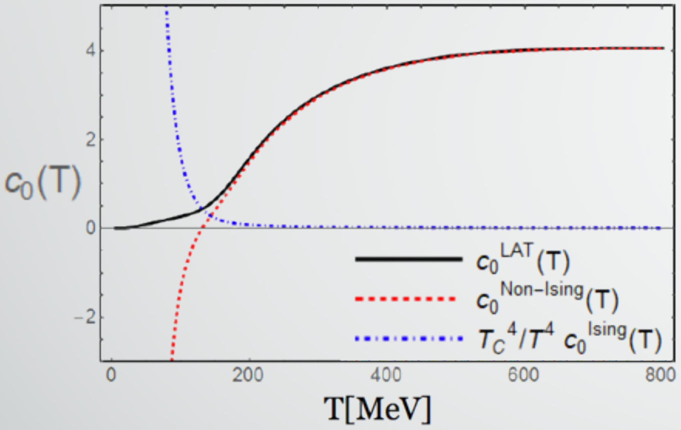

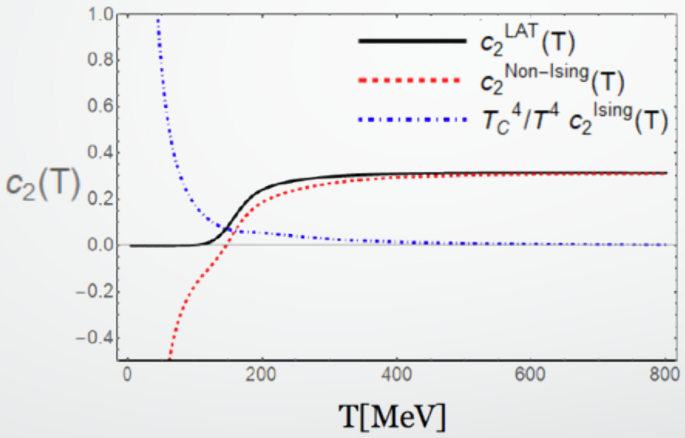

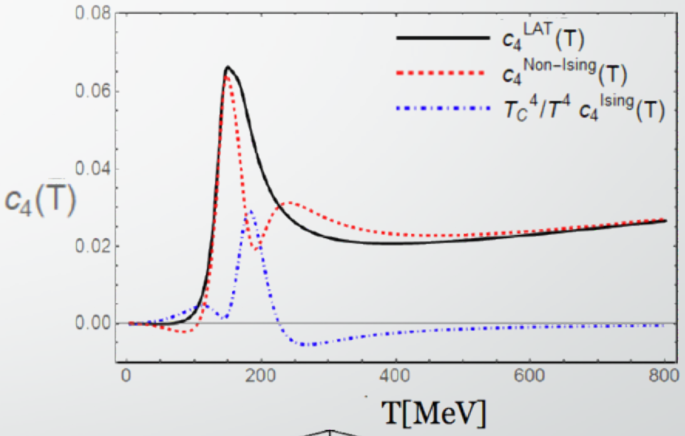

Total pressure becomes:

$$P(T,\mu_B) = T^4 \sum_n c^n_{\text{Non-Ising}}(T) \left(\frac{\mu_B}{T}\right)^n + T_C^4 P_{\mathrm{Ising}}(T,\mu_B)$$

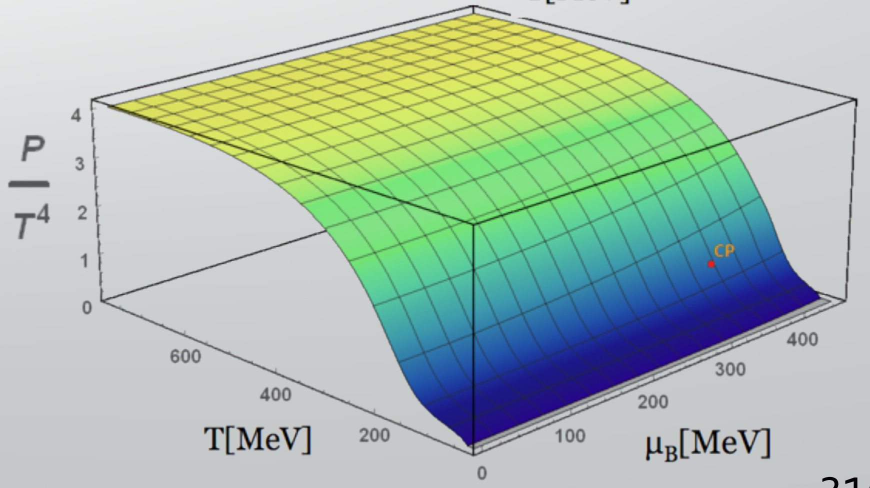

Merging with the HRG model at low T

$\Rightarrow$ **Smooth merging with Hadron Resonance Gas (HRG) model through:**

$$\frac{P_{\mathrm{Final}}(T,\mu_B)}{T^4} = \frac{P(T,\mu_B)}{T^4}\frac{1}{2}\left[1+\tanh\left(\frac{T-T'(\mu_B)}{\Delta T}\right)\right] + \frac{P_{\mathrm{HRG}}(T,\mu_B)}{T^4}\frac{1}{2}\left[1-\tanh\left(\frac{T-T'(\mu_B)}{\Delta T}\right)\right]$$

where:

- $T'(\mu_B)$ is the "transition" temperature, depending on μ_B:

$$T'(\mu_B) = T_0 + \frac{\kappa}{T_0}\mu_B^2 - T^*$$

- ΔT is a measure of the overlap region size

$\Rightarrow$ **In the following:** $T^* = 23\,\mathrm{MeV}$, $\Delta T = 17\,\mathrm{MeV}$

Final EoS: Thermodynamic quantities

Once the pressure is determined, all thermodynamic quantities can be calculated:

Entropy density : $$\frac{S}{T^3} = \frac{1}{T^3}\frac{\partial P}{\partial T}$$

Baryon density : $$\frac{n_B}{T^3} = \frac{1}{T^3}\frac{\partial P}{\partial \mu_B}$$

Energy density : $$\frac{\epsilon}{T^4} = \frac{S}{T^3} - \frac{P}{T^4} + \frac{\mu_B}{T}\frac{n_B}{T^3}$$

Speed of sound : $$c_s^2 = \left(\frac{\partial P}{\partial \epsilon}\right)_{s/n_B} = \frac{n_B^2 \partial_T^2 P - 2 S n_B \partial_T \partial_{\mu_B} P + S^2 \partial_{\mu_B}^2 P}{(\epsilon + P)\left(\partial_T^2 P \partial_{\mu_B}^2 P - (\partial_T \partial_{\mu_B} P)^2\right)}$$

Baryon susceptibilities : $$\chi_n^B = \frac{\partial (P/T^4)}{\partial (\mu_B/T)}$$ (only the second one in the paper)

Final EoS: Pressure and Entropy Density

P. Parotto et al.,: PRC (2020)

The final EoS covers the range:

$$T = 30 - 800\,\mathrm{MeV} \qquad \mu_B = 0 - 450\,\mathrm{MeV}$$

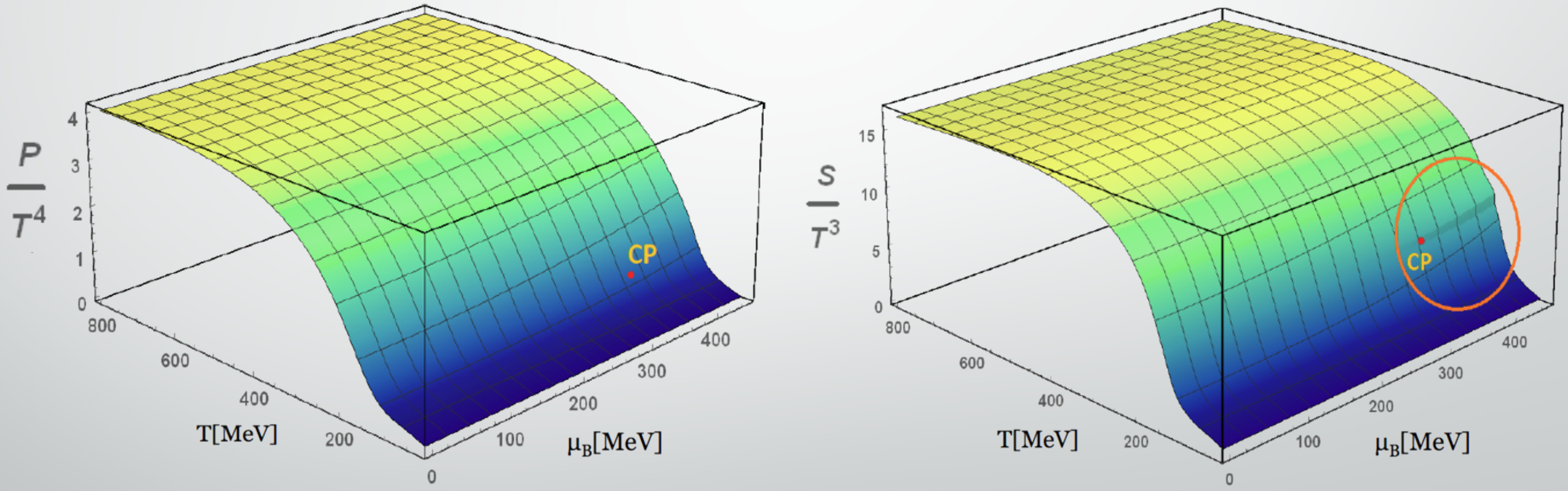

Although the effect is barely visible in the pressure, the entropy density shows a discontinuity in the first order transition region.

Final EoS: Baryon and Energy Density

P. Parotto et al.,: PRC (2020)

The final EoS covers the range:

$$T = 30 - 800\,\text{MeV} \qquad \mu_B = 0 - 450\,\text{MeV}$$

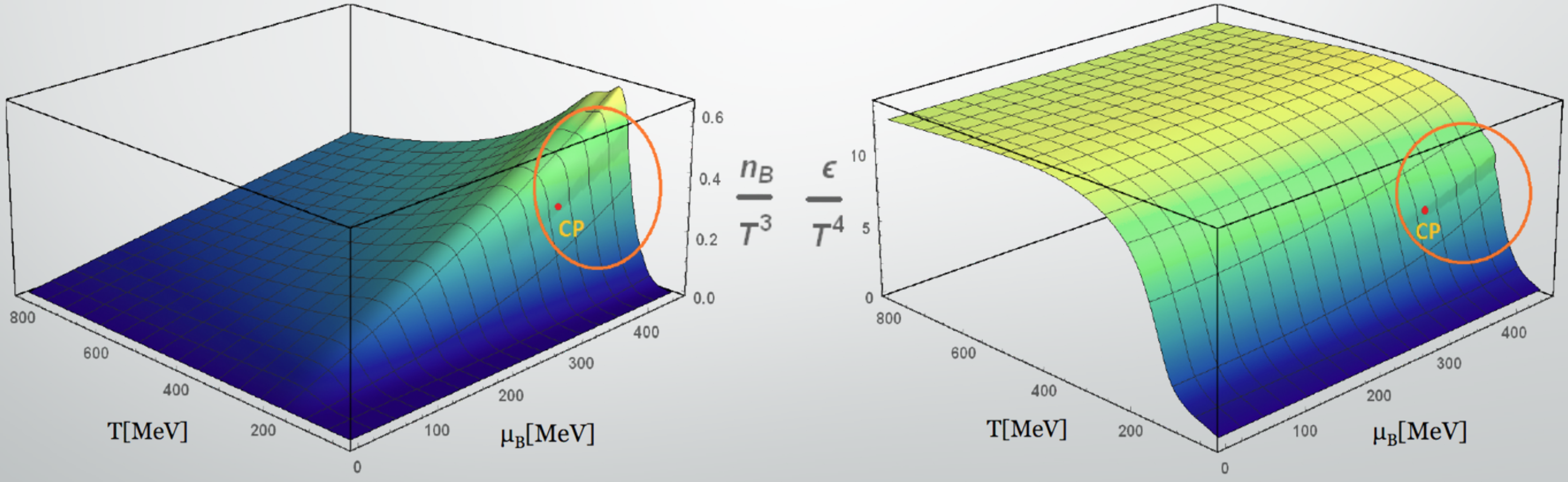

Baryon and energy density also show a discontinuity in the first order transition region.

Final EoS: Speed of sound and baryon number χ_2

P. Parotto et al.,: PRC (2020)

The final EoS covers the range:

$$T = 30 - 800\,\mathrm{MeV} \qquad \mu_B = 0 - 450\,\mathrm{MeV}$$

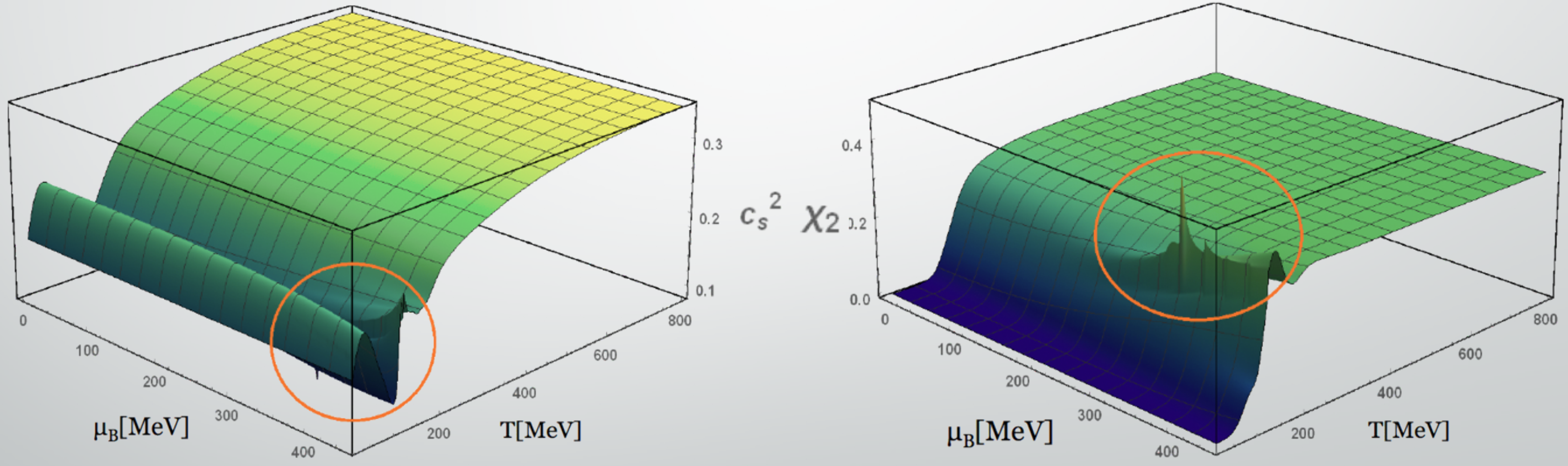

The speed of sound and the second baryon number cumulant show a (weak) dip and a (strong) peak at the critical point respectively.

Final EoS: isentropic trajectories

P. Parotto et al.,: PRC (2020)

- Relevant for hydrodynamic evolution are the lines of $s/n_B = \text{const}$:
  - Low-μ_B: match behavior from Lattice QCD
  - Close to the CP: some structure appears

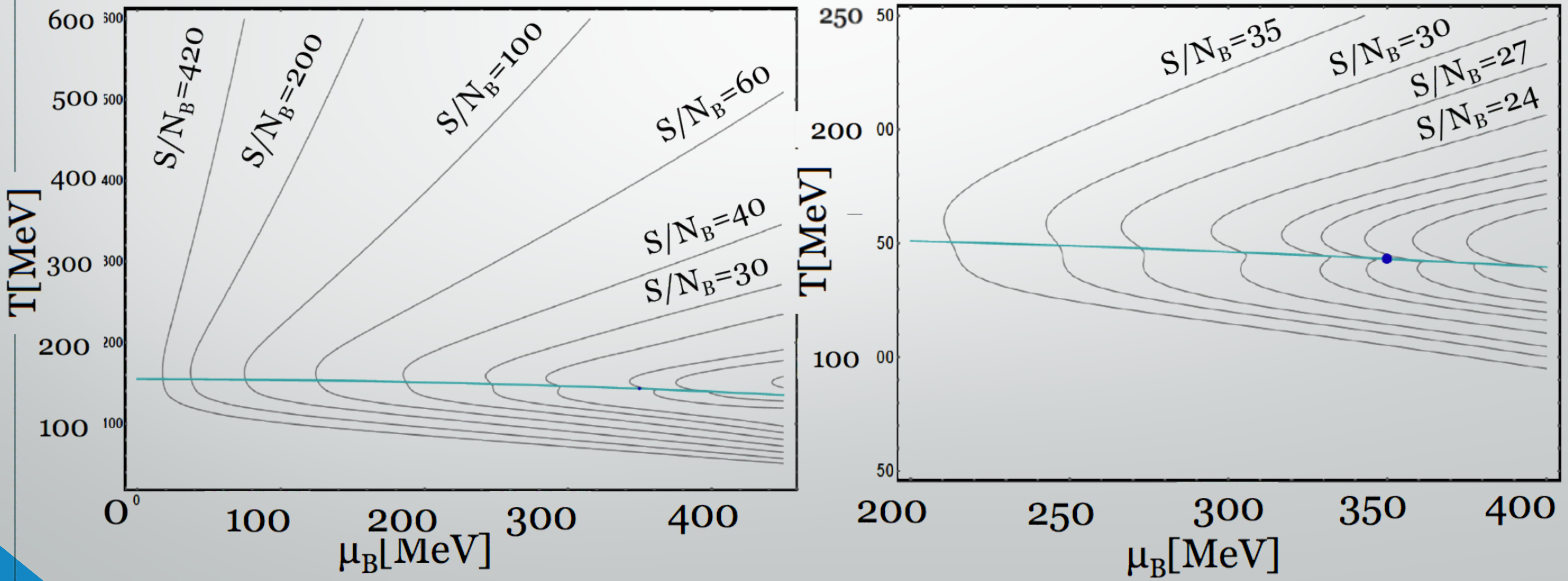

Final EoS: explore parameter space

Keeping the position of the critical point fixed, as well as the orientation of the axes mapped from the 3D Ising model phase diagram, we varied the parameters w, ρ, and required thermodynamic stability $(P, S, n_B, \epsilon, c_s^2 > 0)$ and causality $(c_s^2 \leq 1)$

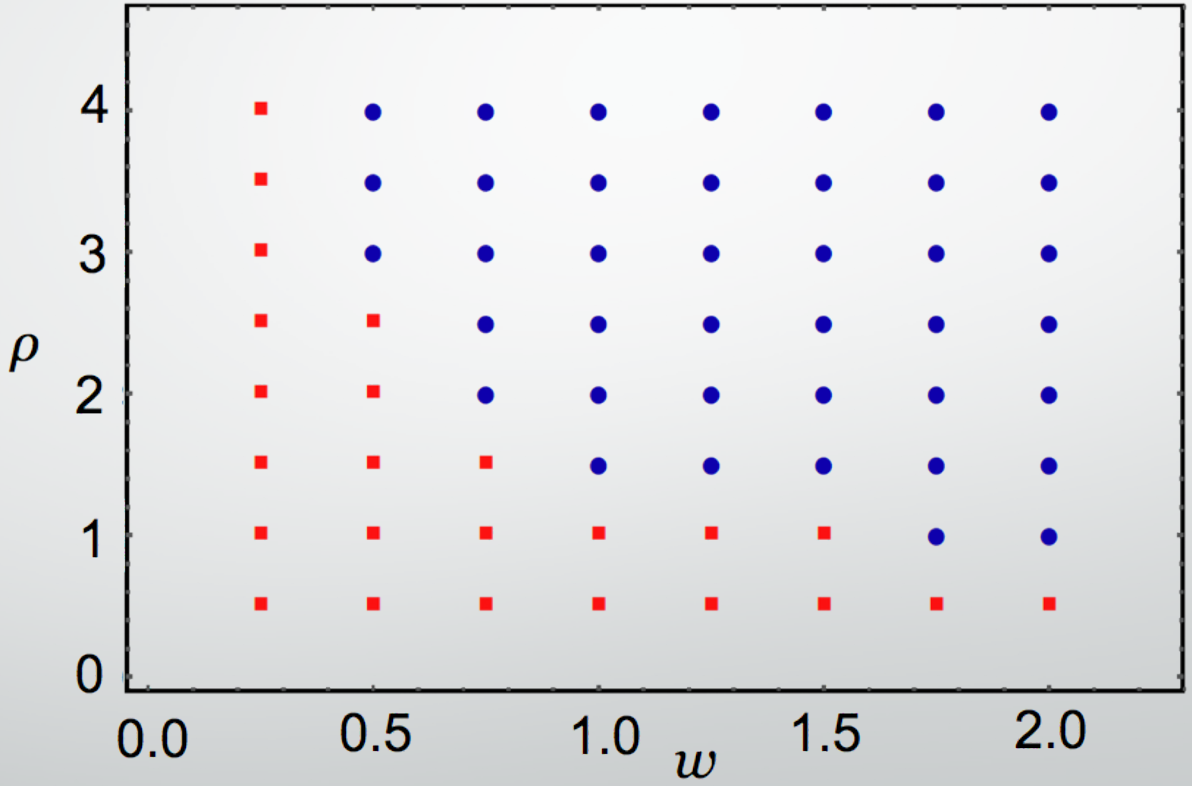

In blue (dots) the values corresponding to acceptable choices, in red (squares) the values leading to pathological EoS's

Behavior of the kurtosis

M. Stephanov, PRL (2011)

- Motivation: predicted behavior of the kurtosis in the vicinity of the critical point:

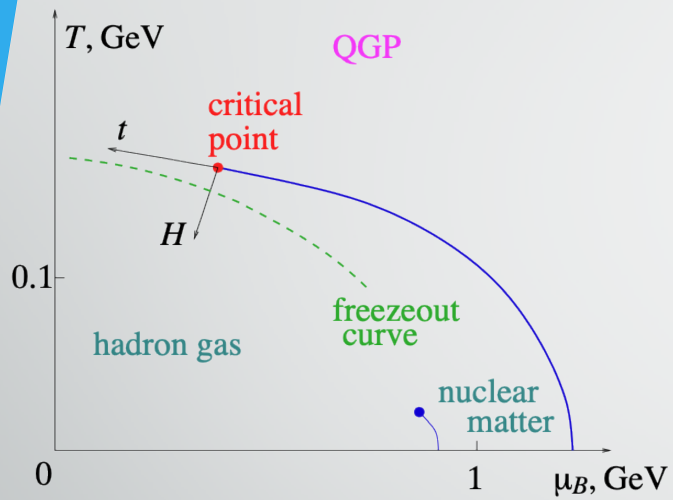

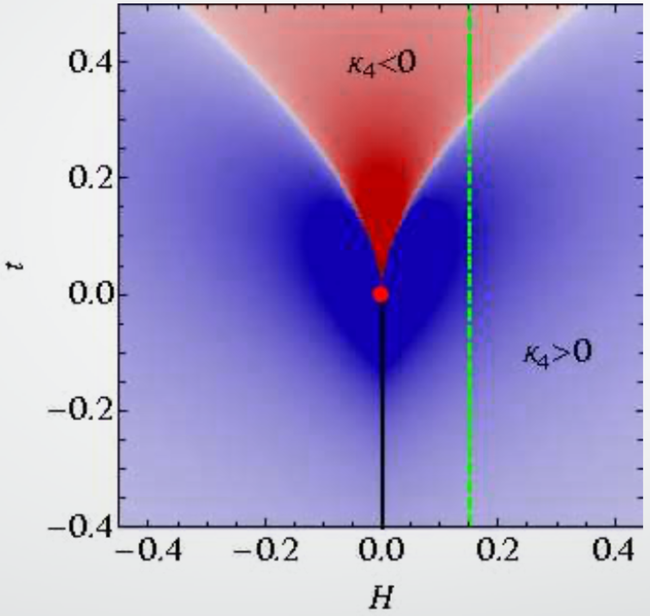

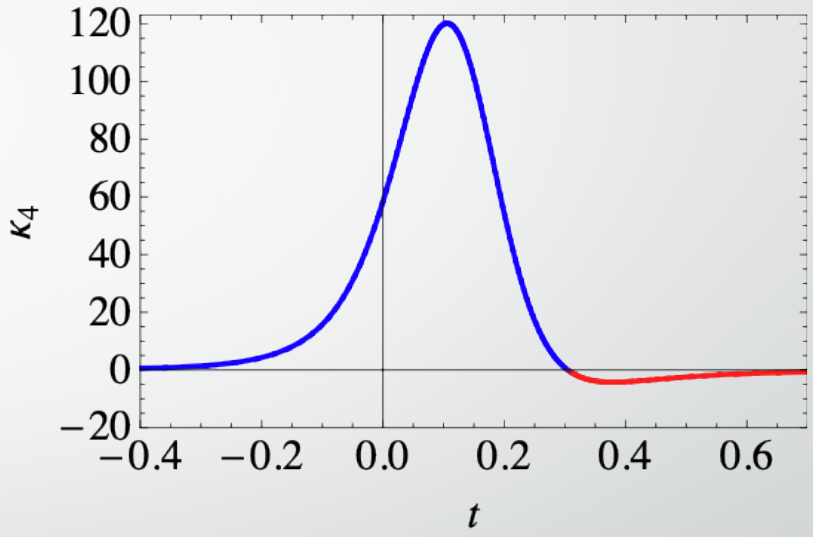

- This behavior was found considering the leading contribution to the kurtosis:

$$\kappa(t,h) = \left(\frac{\partial^3 M}{\partial h^3}\right)_t$$

Behavior of the kurtosis

P. Parotto, C. R. et al., PRC (2020)

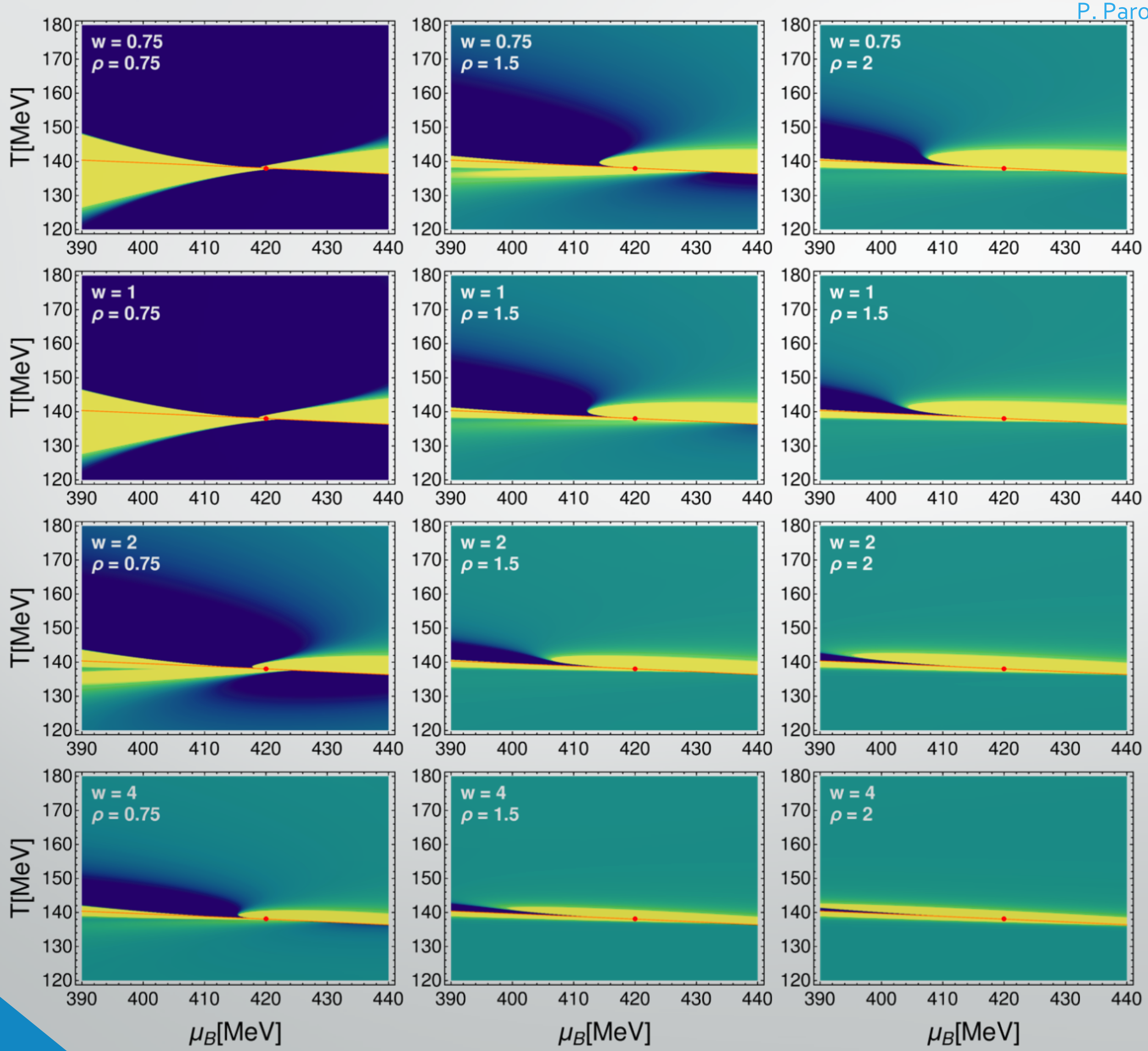

- We can now evaluate all contributions and see whether expected behavior still holds
- The blue area corresponds to negative values
- The blue area is pushed above the transition line
- The dip is difficult to detect at the freeze-out

Implications for the experimental measurement

P. Parotto, C. R. et al., PRC (2020)

- Two sets of parameters

	μ_{BC}	T_C	α_1	$\alpha_2-\alpha_1$	w	ρ
I.	420 MeV	138 MeV	4.6°	$\boxed{90°}$	0.5, 1, 2	0.5, 1, 2
II.	420 MeV	138 MeV	4.6°	$\boxed{-3°}$	0.5, 1, 2	0.5, 1, 2

Common choice in literature. Orthogonal axes.

Motivated by M.S. Pradeep, M. Stephanov, Phys. Rev. D 100 (2019)

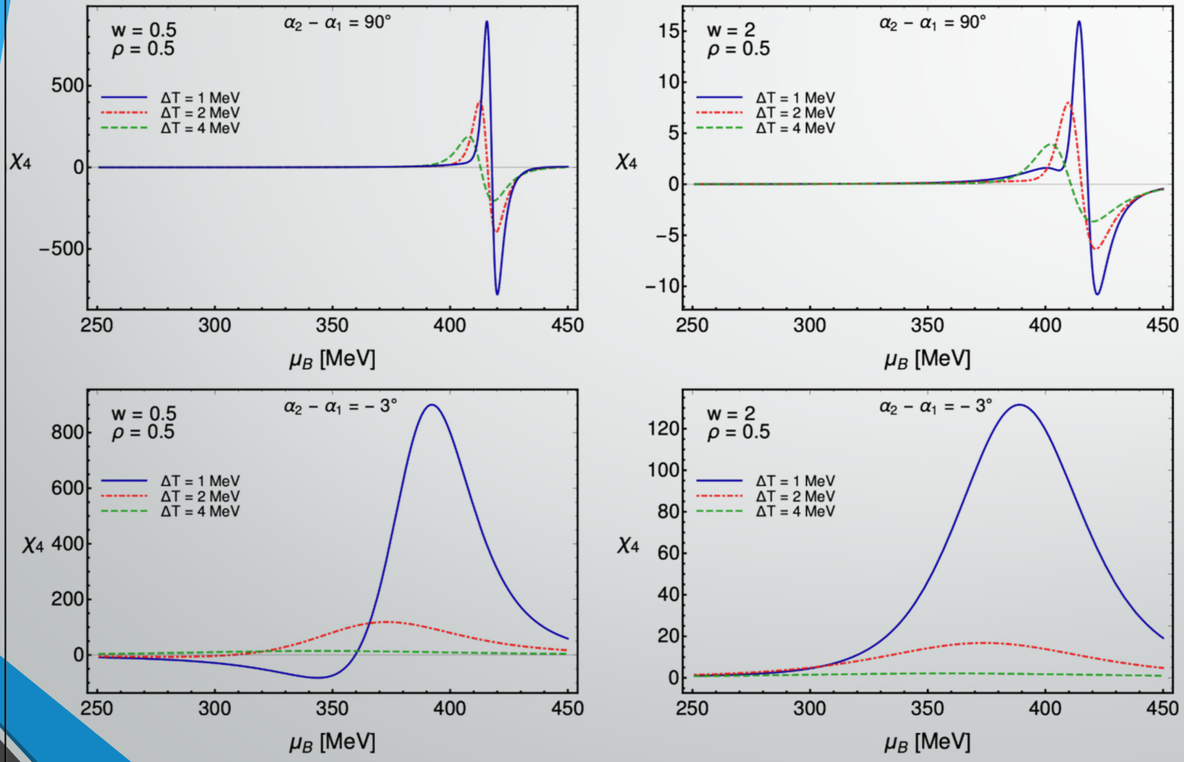

- **Assume** net-proton kurtosis follows critical behavior of χ_4^B.
- Take exemplary freeze-out lines parallel to chiral transition:

$$T_F(\mu_B) = T_0 + \kappa_2 T_0 \left(\frac{\mu_B}{T_0}\right)^2 - \Delta T$$

- Dip only appears for one choice, close to the vicinity of the transition line.

Strangeness-neutral EoS

Collaborators: Jamie Karthein, Angel Nava Acuna, Damien Price (UH), Paolo Parotto (University of Wuppertal), Debora Mroczek, Jaki Noronha-Hostler (UIUC)

New version of the code can be downloaded at:
https://bitbucket.org/bestcollaboration/eos_with_critical_point/src/master/

New version

J. Karthein, C. R. et al., EPJPlus (2021)

- New version includes (but not limited to):
  - Imposing conditions on conserved charges as present in HICs
  - Hadronic species present in SMASH hadronic transport approach

$$\langle n_S \rangle = 0 \qquad\qquad \langle n_Q \rangle = 0.4 \langle n_B \rangle$$

Degrees of Freedom

N	Δ	Λ	Σ	Ξ	Ω	Unflavored				Strange
N_{938}	Δ_{1232}	Λ_{1116}	Σ_{1189}	Ξ_{1321}	Ω^-_{1672}	π_{138}	$f_{0\,980}$	$f_{2\,1275}$	$\pi_{2\,1670}$	K_{494}
N_{1440}	Δ_{1620}	Λ_{1405}	Σ_{1385}	Ξ_{1530}	Ω^-_{2250}	π_{1300}	$f_{0\,1370}$	$f'_{2\,1525}$		K^*_{892}
N_{1520}	Δ_{1700}	Λ_{1520}	Σ_{1660}	Ξ_{1690}		π_{1800}	$f_{0\,1500}$	$f_{2\,1950}$	$\rho_{3\,1690}$	$K_{1\,1270}$
N_{1535}	Δ_{1900}	Λ_{1600}	Σ_{1670}	Ξ_{1820}			$f_{0\,1710}$	$f_{2\,2010}$		$K_{1\,1400}$
N_{1650}	Δ_{1905}	Λ_{1670}	Σ_{1750}	Ξ_{1950}		η_{548}		$f_{2\,2300}$	$\phi_{3\,1850}$	K^*_{1410}
N_{1675}	Δ_{1910}	Λ_{1690}	Σ_{1775}	Ξ_{2030}		η'_{958}	$a_{0\,980}$	$f_{2\,2340}$		$K_0^*{}_{1430}$
N_{1680}	Δ_{1920}	Λ_{1800}	Σ_{1915}			η_{1295}	$a_{0\,1450}$		$a_{4\,2040}$	$K_2^*{}_{1430}$
N_{1700}	Δ_{1930}	Λ_{1810}	Σ_{1940}			η_{1405}		$f_{1\,1285}$		K^*_{1680}
N_{1710}	Δ_{1950}	Λ_{1820}	Σ_{2030}			η_{1475}	ϕ_{1019}	$f_{1\,1420}$	$f_{4\,2050}$	$K_{2\,1770}$
N_{1720}		Λ_{1830}	Σ_{2250}				ϕ_{1680}			$K_3^*{}_{1780}$
N_{1875}		Λ_{1890}				σ_{800}		$a_{2\,1320}$		$K_{2\,1820}$
N_{1900}		Λ_{2100}					$h_{1\,1170}$			$K_4^*{}_{2045}$
N_{1990}		Λ_{2110}				ρ_{776}		$\pi_{1\,1400}$		
N_{2060}		Λ_{2350}				ρ_{1450}	$b_{1\,1235}$	$\pi_{1\,1600}$		
N_{2080}						ρ_{1700}				
N_{2100}							$a_{1\,1260}$	$\eta_{2\,1645}$		
N_{2120}						ω_{783}				
N_{2190}						ω_{1420}		$\omega_{3\,1670}$		
N_{2220}						ω_{1650}				
N_{2250}										

As of SMASH-1.7

- + corresponding antiparticles
- Perturbative treatment of photons and dileptons
- Isospin symmetry

- Mesons and baryons according to particle data group
- Isospin multiplets and anti-particles are included

H. Elfner, RHIC-BES Seminar (2020)
J. Weil et al, PRC (2016)

Taylor coefficients from lattice QCD

J. Karthein, C. R. et al., EPJPlus (2021)

➤ Lattice results for Taylor expansion of pressure around $\mu_B = 0$ up to $\mathcal{O}(\mu_B^4)$ are the backbone of the procedure for creating this equation of state

$$\frac{P(T,\mu_B)}{T^4} = \sum_n c_{2n}(T)\left(\frac{\mu_B}{T}\right)^{2n}$$

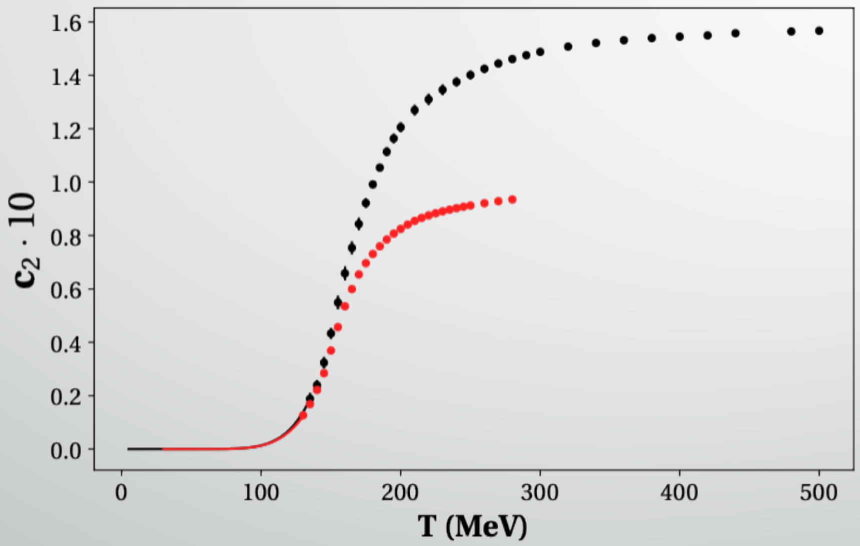

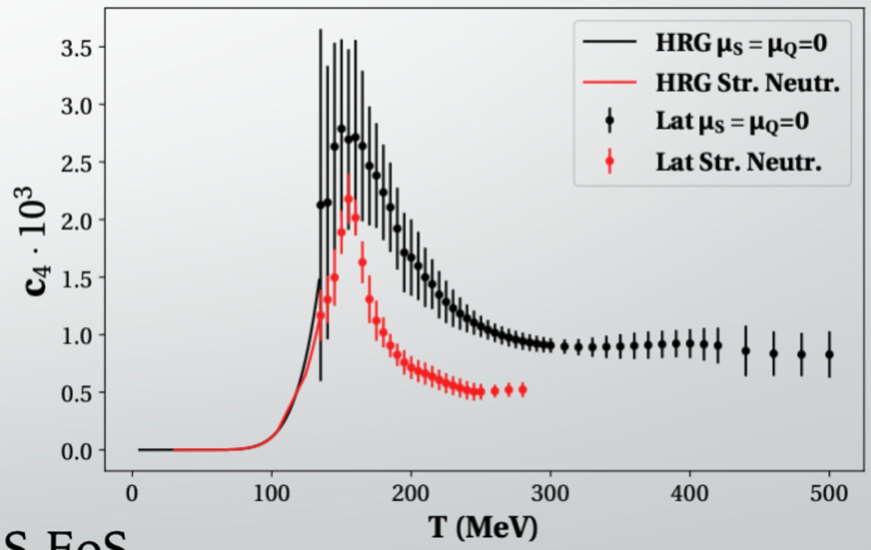

— original BES-EoS

— updated version

J. Guenther et al, NPA (2017)
R. Bellweid et al, PRD (2015)
See also: A. Bazavov et al, PRD (2017)

Lattice mode

J. Karthein, C. R. et al., EPJPlus (2021)

➤ Strangeness neutral equation of state from first-principles can be produced by running in "LAT" mode

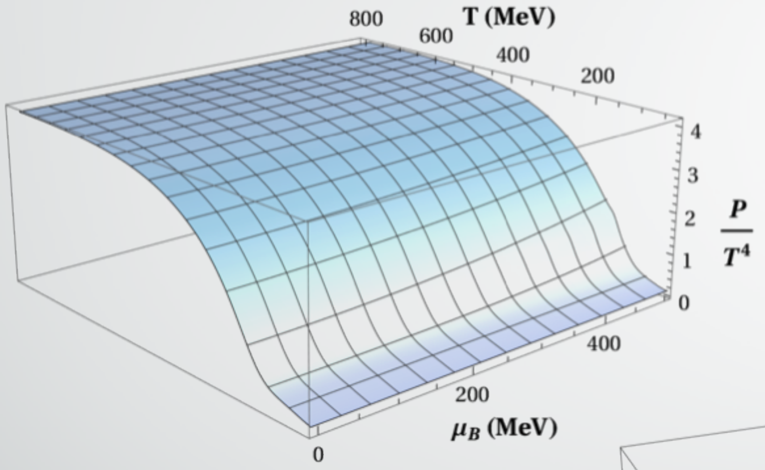

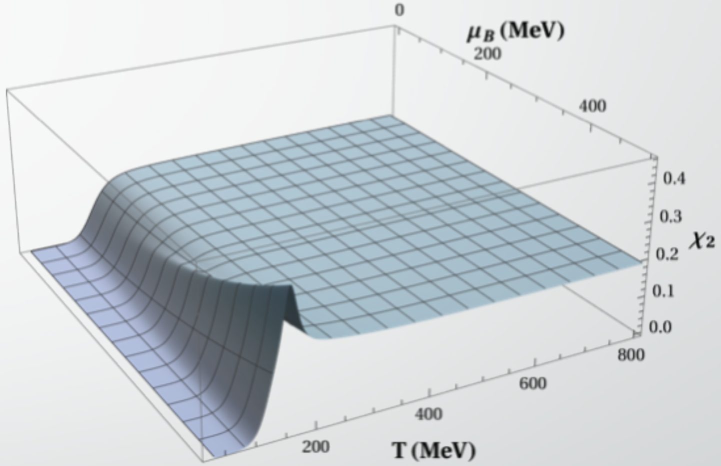

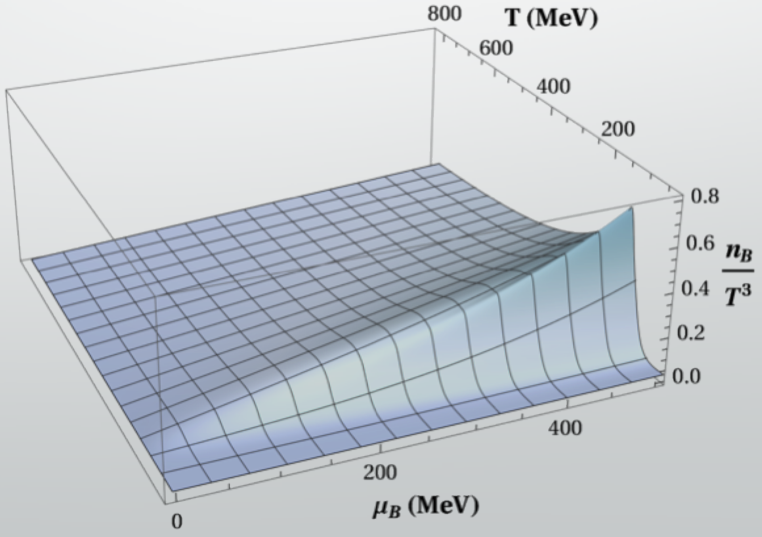

Equation of state

J. Karthein, C. R. et al., EPJPlus (2021)

- Pressure and its derivatives show effects of critical region on these quantities: stronger effects with increasing derivatives

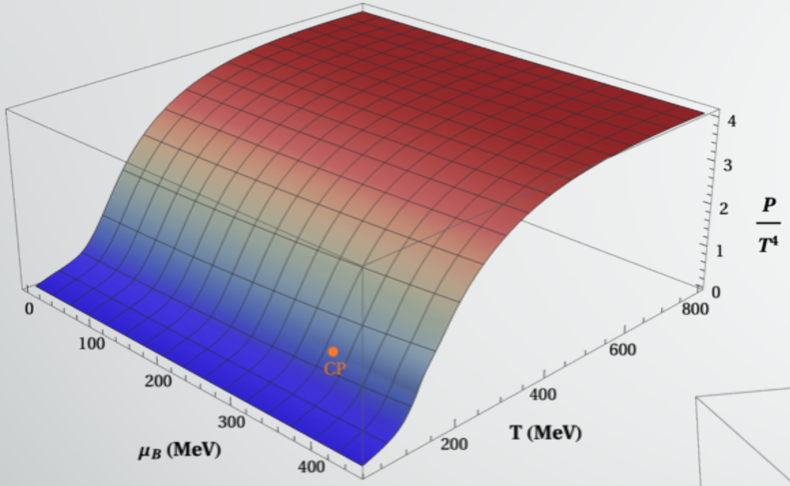

Pressure

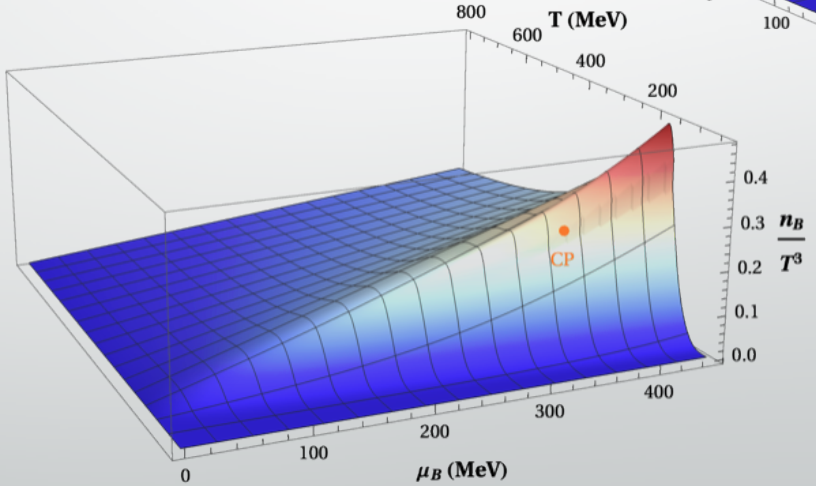

Baryon density

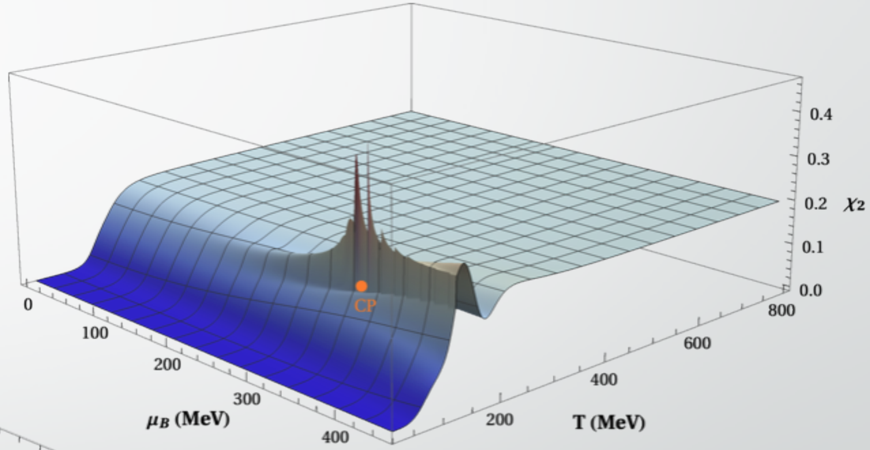

χ_2^B

JS et al, arXiv:2103.08146

Equation of state

J. Karthein, C. R. et al., EPJPlus (2021)

➤ Energy density and entropy exhibit discontinuities, while the speed of sound approaches zero at the critical point

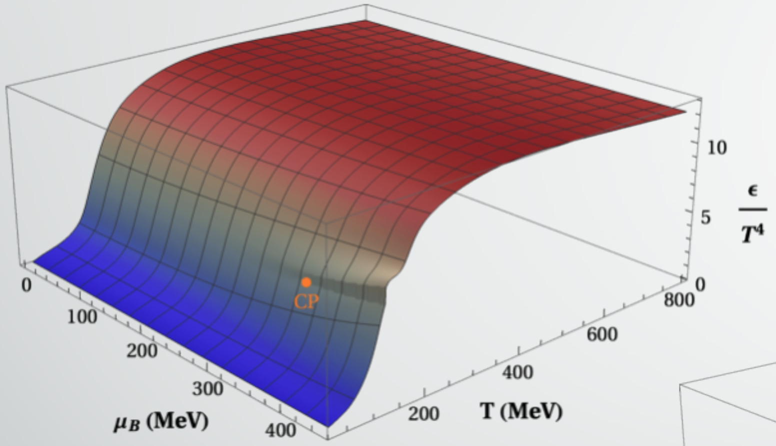

Energy density

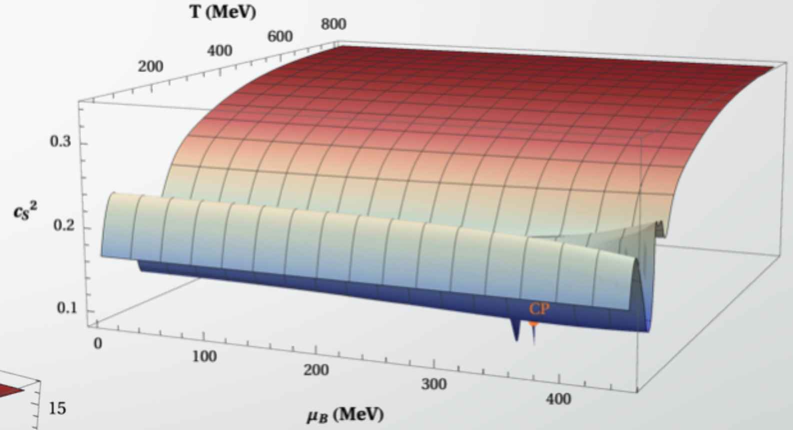

Speed of sound

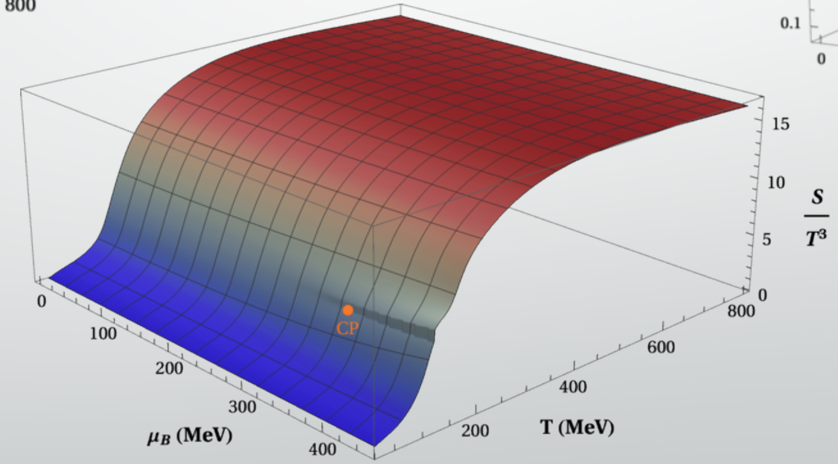

Entropy

Equation of state differences

J. Karthein, C. R. et al., EPJPlus (2021)

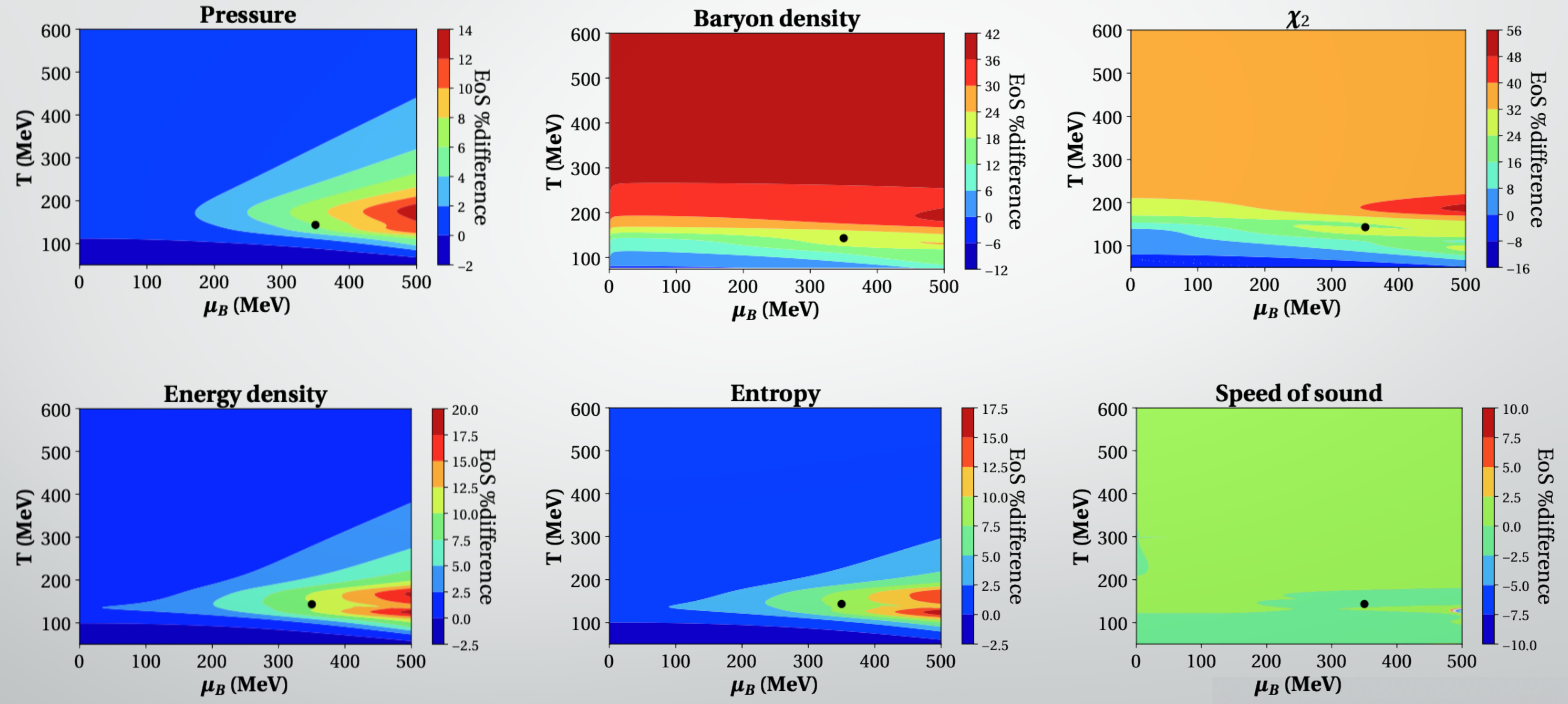

Differences in isentropic trajectories

J. Karthein, C. R. et al., EPJPlus (2021)

- Isentropes show the path of the HIC system through the phase diagram in the absence of dissipation
  - Different path when conserved charge conditions applied

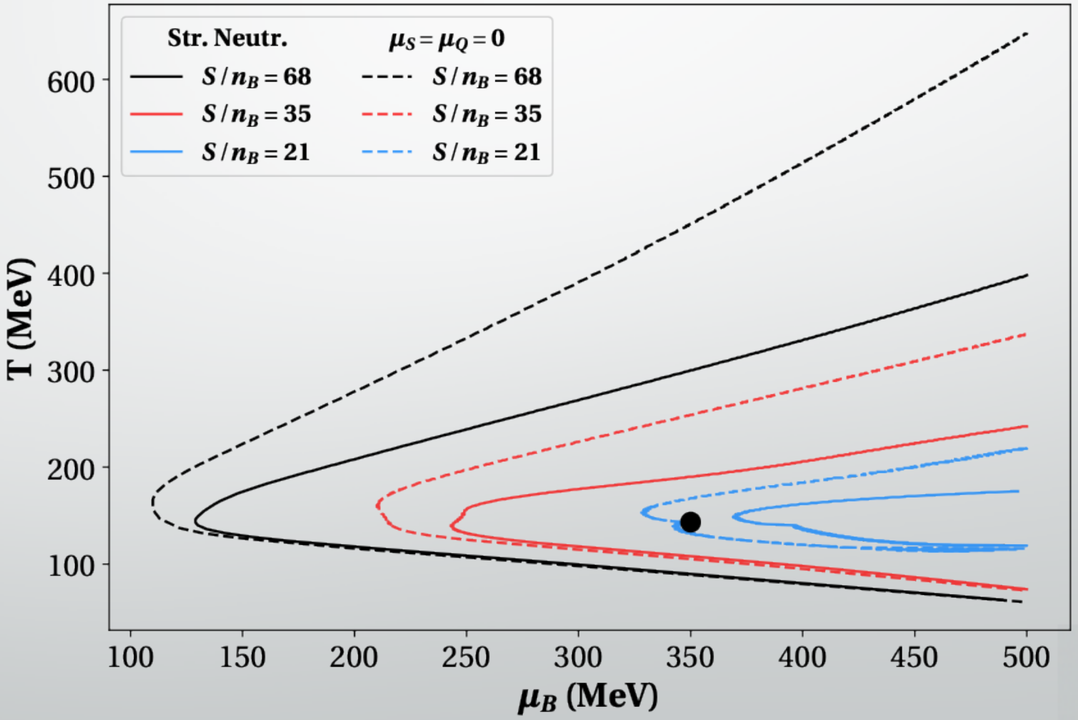

Conclusions

- From lattice QCDTaylor expansionwe currently have the EoS for $\mu_B/T<2$
- We constructed a family of Equations of State containing a Critical Point in the 3D Ising model universality class to study its effect
- The dip in the kurtosis is very difficult to observe at the chemical freeze-out
- We recently extended the EoS to the case of strangeness neutrality